J. Mol. Biol. (1998) **277**, 1091–1110

JMB

Folding of β-Sheet Membrane Proteins: A Hydrophobic Hexapeptide Model

William C. Wimley[1], Kalina Hristova[1], Alexey S. Ladokhin[1] Loraine Silvestro[2], Paul H. Axelsen[2] and Stephen H. White[1]*

[1]*Department of Physiology and Biophysics, University of California, Irvine, CA 92697-4560, USA*

[2]*Department of Pharmacology Johnson Foundation for Molecular Biophysics University of Pennsylvania Philadelphia, PA 19104-6084 USA*

**Corresponding author*

Beta-sheets, in the form of the β-barrel folding motif, are found in several constitutive membrane proteins (porins) and in several microbial toxins that assemble on membranes to form oligomeric transmembrane channels. We report here a first step towards understanding the principles of β-sheet formation in membranes. In particular, we describe the properties of a simple hydrophobic hexapeptide, acetyl-Trp-Leu_5 ($AcWL_5$), that assembles cooperatively into β-sheet aggregates upon partitioning into lipid bilayer membranes from the aqueous phase where the peptide is strictly monomeric and random coil. The aggregates, containing 10 to 20 monomers, undergo a relatively sharp and reversible thermal unfolding at ~60°C. No pores are formed by the aggregates, but they do induce graded leakage of vesicle contents at very high peptide to lipid ratios. Because β-sheet structure is not observed when the peptide is dissolved in *n*-octanol, trifluoroethanol or sodium dodecyl sulfate micelles, aggregation into β-sheets appears to be an exclusive property of the peptide in the bilayer membrane interface. This is an expected consequence of the hypothesis that a reduction in the free energy of partitioning of peptide bonds caused by hydrogen bonding drives secondary structure formation in membrane interfaces. But, other features of interfacial partitioning, such as side-chain interactions and reduction of dimensionality, must also contribute. We estimate from our partitioning data that the free energy reduction per residue for aggregation is about 0.5 kcal mol^{-1}. Although modest, its aggregate effect on the free energy of assembling β-sheet proteins can be huge. This surprising finding, that a simple hydrophobic hexapeptide readily assembles into oligomeric β-sheets in membranes, reveals the potent ability of membranes to promote secondary structure in peptides, and shows that the formation of β-sheets in membranes is more facile than expected. Furthermore, it provides a basis for understanding the observation that membranes promote self-association of β-amyloid peptides. $AcWL_5$ and related peptides thus provide a good starting point for designing peptide models for exploring the principles of β-sheet formation in membranes.

Keywords: β-barrel proteins; β-amyloid peptides; partitioning of peptides into membranes; lipid bilayers; thermal unfolding

Present address: A. S. Ladohkin, Palladin Institute of Biochemistry, National Academy of Sciences of Ukraine, Kiev, 252030, Ukraine.

Abbreviations used: DOPC, 1,2-dioleoyl-*sn*-glycero-3-phosphocholine; OBPC, 1-oleoyl-2-(9,10-dibromostearoyl)-*sn*-glycero-3-phosphocholine; DMPC, 1,2-dimyristoyl-*sn*-glycero-3-phosphocholine; ANTS, 8-aminonaphthalene-1,3,6 trisulfonic acid, 427.33 Da; DPX, *p*-xylene-bis-pyridinium bromide, 422.16 Da; PATIR-FTIR, Polarized attenuated total internal reflection Fourier transform infrared; $AcWL_5$, acetyl-Trp-Leu_5; LUV, large unilamellar vesicles; TFE, trifluoroethanol.

0022–2836/98/151091–20 $25.00/0/mb981640

Introduction

The folding of proteins into membranes can occur spontaneously, as for pore-forming toxins (Gouaux, 1997), or through a series of protein-catalyzed steps as for constitutive membrane proteins (Simon, 1995; Do *et al*., 1996). In either case, the folded protein is presumably in a free-energy minimum determined by numerous interactions of the protein chain(s) with the membrane, other chain segments, and water. The fundamental principles of protein stability in membranes can be addressed through consideration of three conceptual folding steps (Jacobs & White, 1989): Binding to the membrane interface, formation of secondary structure, and insertion of secondary-structure elements into the membrane. A critical feature of this conceptual model of folding and stability is the propensity of membranes to promote secondary structure formation that we refer to as partitioning-folding coupling (Wimley & White, 1996). This well-known property has been demonstrated for a wide variety of peptides that gain α-helical content upon binding to membranes (Kanellis *et al*., 1980; Kaiser & Kezdy, 1983; Tamm *et al*., 1989; Wang *et al*., 1993; Tytler *et al*., 1995) and has, in a few cases, been studied systematically (Cornut *et al*., 1994; Li & Deber, 1994; Deber & Li, 1995; Dathe *et al*., 1996; Kiyota *et al*., 1996). There are also a few unrelated examples of peptides that form β-sheet structure in membranes (Cornell *et al*., 1989; Krantz *et al*., 1991; Lee *et al*., 1995; Aggeli *et al*., 1996). Wimley & White (1996) have shown that the high free energy cost of partitioning peptide bonds dominates the energetics of the partitioning of amino acid residues into the bilayer interface. They have hypothesized that secondary structure formation is driven, in part, by a reduction in the free energy of peptide-bond partitioning that accompanies hydrogen bond formation. The work presented here is consistent with that hypothesis.

Studies of the folding and insertion of the β-sheet proteins OmpA and OmpF into model membranes have been reported by several laboratories (Dornmair *et al*., 1990; Eisele & Rosenbusch, 1990; Kleinschmidt & Tamm, 1996; Surrey *et al*., 1996). The general approach used was to initiate folding by diluting a solution of protein prepared by solubilization with urea or detergents. Here, we describe a simple model system for studying β-sheet formation in membranes that does not require urea or detergents. Specifically, we present the results of studies of the membrane partitioning and folding of a simple hydrophobic hexapeptide, acetyl-Trp-Leu$_5$ ($AcWL_5$), that helps clarify the general principles of induction of secondary structure by membranes. Even though the peptide is a monomeric random coil in the aqueous phase, it aggressively and cooperatively assembles reversibly into β-sheet aggregates when partitioned into membranes. An important feature of the system is that the aggregates can be reversibly unfolded at moderate temperatures.

A simple system for studying β-sheet formation in membranes is significant because the β-barrel is turning out to be an important motif of membrane proteins (Schulz, 1996) and pore-forming toxins (Gouaux, 1997). Although $AcWL_5$ is not an amphipathic strand and does not apparently form β-barrels (see below), it nevertheless provides important insights into the energetics of assembling β-barrels in membranes. The known β-barrels are all pore-forming proteins composed of 14 (Song *et al*., 1996), 16 (Weiss *et al*., 1991) or 18 (Schirmer *et al*., 1995) transmembrane anti-parallel β-strands twisted around a central channel axis. These include the single-chain porins (Schulz, 1996), constitutive membrane proteins that are found in bacterial outer membranes, and α-hemolysin toxin from *Staphylococcus aureus* (Gouaux, 1997) that assembles on membranes into heptameric transmembrane pores. Other probable β-barrel membrane proteins include the mitochondrial VDAC channel (Mannella, 1992), the protein toxin aerolysin (Parker *et al*., 1994), and the anthrax protective antigen (Petosa *et al*., 1997). β-Sheet formation on membranes has been implicated in the initiation of β-amyloid fibril formation (Terzi *et al*., 1994b, 1995; Yanagisawa *et al*., 1995; Fletcher & Keire, 1997) and β-amyloid neurotoxicity (Nitsch *et al*., 1992; Svennerholm & Gottfries, 1994; McLaurin & Chakrabartty, 1996).

We first describe the cooperative partitioning of $AcWL_5$ and other members of the $AcWL_n$ family of peptides into membranes, the kinetics of peptide aggregation, and formation of secondary structure by the aggregates. We then address in turn the effect of temperature on partitioning and β-sheet formation and the effect of $AcWL_5$ aggregates on membrane permeability. The results reveal the unexpected ease of membrane-induced β-sheet formation and demonstrate the potential usefulness of $AcWL_5$ and related peptides for understanding the folding of β-sheets in membranes.

Results

The partitioning and secondary structure formation of $AcWL_5$ were examined using large unilamellar vesicles (LUV) formed by extrusion (Mayer *et al*., 1986), primarily from palmitoyloleoylphosphatidylcholine (POPC). For reasons discussed below, we also used LUV formed from 1-oleoyl-2-(9,10-dibromostearoyl)-*sn*-glycero-3-phosphocholine (OBPC) for examining the cooperative assembling of β-sheet aggregates. We also made a limited number of measurements using $AcWL_4$, $AcWL_4$-*O*-methyl, $AcWL_6$, $AcWL_7$ and $AcWL_8$. A homologous peptide, AcWLWLL, which is very similar to $AcWL_5$ in sequence, length and hydrophobicity, but which binds to membranes as a monomeric random coil under all conditions (Wimley *et al*., 1996; Wimley & White, 1996), was used as a control peptide. Partitioning into POPC LUV was measured using equilibrium dialysis

(Wimley & White, 1993b, 1996; White *et al.*, 1997; Ladokhin *et al.*, 1997a), while for OBPC a centrifugation method was used (White *et al.*, 1997). Aggregation/polymerization reactions in bulk phases are generally followed by measuring the concentrations of aggregates of all sizes as a function of total protomer concentration. Here, we follow aggregation on the membrane by plotting the apparent mole-fraction partition coefficient of the peptide, K_x^a, against the membrane concentration expressed as the bound-peptide to lipid ratio, *P*:*L* (see Materials and Methods). K_x^a approaches the monomer value K_x at low $P:L$ values. Two fundamental facts about $AcWL_5$ should be kept in mind throughout this work: (1) $AcWL_5$ is monomeric in water at all concentrations at which it is soluble; and (2) its conformation as a monomer in water is random coil as judged by circular dichroism (CD) spectroscopy (Wimley *et al.*, 1996; Wimley & White, 1996). This means that equilibration between aqueous and membrane-bound peptide occurs through partitioning of random-coil monomers.

Cooperative membrane partitioning of $AcWL_5$

The first indication that $AcWL_5$ has unexpected properties in membranes came from equilibrium dialysis experiments in which we observed that its binding to POPC vesicles increased sharply with concentration, suggestive of a cooperative process (Wimley & White, 1996). Generally, the partition coefficients K_x for small hydrophobic peptides similar to $AcWL_5$ are independent of concentration (Wimley & White, 1996), as shown by the data for AcWLWLL in Figure 1 (open circles). The partitioning of $AcWL_5$ into POPC LUV (filled squares), on the other hand, is independent of concentration only for $P:L < 0.001$ (the concentration range used in our previous report of the binding of this peptide to bilayers, Wimley & White, 1996). Partitioning begins increasing for $P:L > 0.001$ and dramatically so for $P:L > 0.005$, approaching 40 K_x for $P:L \sim 0.03$. This unprecedented increase in partitioning with *P*:*L* suggests a high degree of cooperativity. Cooperative partitioning of small peptides into membranes is unusual, although it has been inferred from studies of some larger peptides (Ludtke *et al.*, 1994; He *et al.*, 1995; Golding *et al.*, 1996; Rapaport *et al.*, 1996).

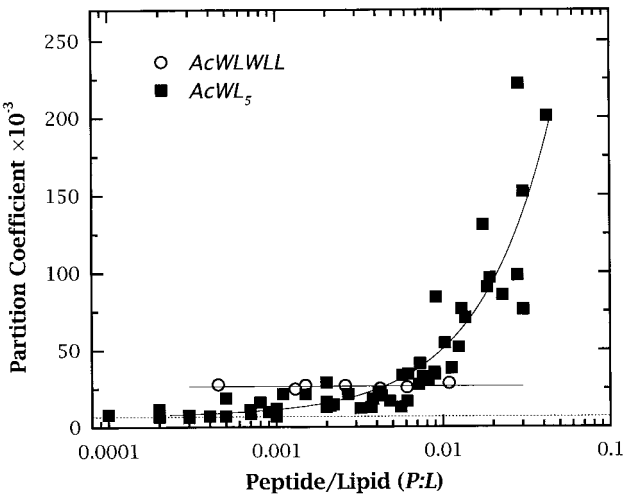

Figure 1. Membrane-concentration dependence of the partitioning of $AcWL_5$ (■) and AcWLWLL (○) into POPC determined using equilibrium dialysis. Partition coefficients are in mole-fraction units (see Materials and Methods). The peptide per lipid ratio (*P*:*L*) is the ratio of the moles of bound peptide per mole of lipid. The partitioning of the control peptide AcWLWLL is independent of concentration. $AcWL_5$, on the other hand, partitions cooperatively because of self-association into aggregates on the membrane. The continuous line is the result of fitting a nucleation-growth model to the binding data (see Results). The broken line represents the expectation for monomeric partitioning.

The related peptide, AWL_6, also shows cooperative partitioning behavior (data not shown), but with higher partition coefficients than $AcWL_5$, as expected from its higher degree of hydrophobicity. Unfortunately, systematic measurements on $AcWL_6$ were impractical because of its low aqueous-phase solubility and its tendency to aggregate in water (Wimley *et al.*, 1996; and see Materials and Methods). The peptides $AcWL_7$ and $AcWL_8$ also appear to form β-sheets in POPC vesicles (data not shown). The peptide $AcWL_4$ apparently does not bind cooperatively to POPC, but its overall weaker binding due to its lower degree of hydrophobicity prevents measurements at sufficiently high *P*:*L* ratios. If the carboxy terminus of $AcWL_4$ is methylated, then binding is much stronger and we observe cooperative formation of β-sheets (data not shown).

Why is the partitioning apparently cooperative? Two simple explanations are: (1) self-association on the membrane that leads to recruitment of monomers from the aqueous phase; or (2) enhanced monomer partitioning due to membrane perturbations. As a test for the second possibility, we examined the effect of the partitioning of $AcWL_5$ on the partitioning of AcWLWLL (the non-aggregating control peptide). This was done by placing AcWLWLL in the dialysis chamber along with concentrations of $AcWL_5$ appropriate for attaining *P*:*L* ratios of either ~0.02 or <0.001. The results, summarized in Table 1, show that the partitioning of AcWLWLL at high $AcWL_5$ *P*:*L* values is decreased about 25% compared to low $AcWL_5$ *P*:*L* values, as expected from simple electrostatic considerations (Stankowski & Schwarz, 1990; Thorgeirsson *et al.*, 1995). On the other hand, the partitioning of $AcWL_5$ increases more than 15-fold, despite the opposing electrostatic effect. These results indicate that high $AcWL_5$ concentrations have not perturbed the membrane to cause a general increase in the partition coefficients of hydrophobic peptides. Self-association of $AcWL_5$ into aggregates is thus the more likely explanation for cooperative partitioning. Kinetic and spectroscopic measurements strongly support this conclusion (see below).

Table 1. Simultaneous partitioning of $AcWL_5$ and AcWLWLL into POPC vesicles

	Concentration (*P*:*L*) of $AcWL_5$ in membrane[a]	
	<0.001[b]	~0.02
AcWLWLL		
$K_x^a \pm$ s.d.[c]	30,000 ± 3500 (12%)	22,100[d] ± 2900 (13%)
No. measurements	10	23
$AcWL_5$		
$K_x^a \pm$ s.d.[c]	7500 ± 1200 (16%)	120,000[d] ± 49,000 (41%)
No. measurements	19	23

[a] Concentration (*P*:*L*) of $AcWL_5$ in the membrane is the ratio of moles of bound $AcWL_5$ to moles of lipid.
[b] In the case of AcWLWLL measured at $AcWL_5$ *P*:*L* <0.001, $AcWL_5$ is absent.
[c] Apparent mole-fraction partition coefficient K_x^a (equation (6)) measured with equilibrium dialysis and HPLC (Wimley & White, 1993b).
[d] In these experiments, the two peptides were present simultaneously in the same samples.

An unexpected feature of the equilibrium dialysis measurements of $AcWL_5$ partitioning, revealed by the data in Table 1, is that the statistical dispersion of K_x^a for $AcWL_5$ at $P{:}L \sim 0.02$ is approximately threefold higher than for $P{:}L < 0.001$ or for K_x^a of AcWLWLL, measured simultaneously at either concentration. The consequence of this increased dispersion is the large experimental variations in $AcWL_5$ partitioning that are apparent in Figure 1. The reasons for this unusual high scatter from a method that generally gives very reproducible results are uncertain. We hypothesized that it arose from a combination of effects, including the slow time-course of $AcWL_5$ aggregation (see below) and relatively long diffusion paths inherent to equilibrium dialysis chambers. To assure ourselves that the experimental scatter was not necessarily a normal feature of aggregation on bilayers, we developed another method for measuring the partitioning of $AcWL_5$ into phosphatidylcholine LUV that permitted equilibration to occur in the absence of a dialysis membrane.

Specifically, we mixed peptide solutions with LUV suspensions and allowed the mixture to come to equilibrium. The total concentration of peptide in the mixture $[P]_{total}$ was then determined by HPLC (see Materials and Methods). Vesicles with bound peptide were subsequently separated from the free peptide by mild centrifugation, and the concentration of free peptide $[P]_{water}$ in the supernatant was determined by HPLC. The apparent partition coefficient was calculated using equation (7); see Materials and Methods. This method is feasible only if the LUV have a specific gravity that is significantly greater than 1. We therefore used LUV formed from OBPC that has a specific gravity of about 1.2 because of the bromine atoms in the *sn*-2 chain. Despite the relatively bulky bromine atoms, the physical properties of brominated lipids are not very different from those of non-brominated lipids (McIntosh & Holloway, 1987; Wiener & White, 1991). Thus, the interactions of peptides with OBPC and POPC LUV are expected to be approximately the same, and this is confirmed by our experiments.

The concentration dependence of $AcWL_5$ partitioning into OBPC LUV, shown in Figure 2, confirms the apparently cooperative nature of the binding of $AcWL_5$ to phosphatidylcholine vesicles and is very similar in concentration dependence and curvature to that for POPC. However, there are two relatively minor differences between the curves shown in Figures 1 and 2 that probably result from differences in the lipids. First, K_x for monomeric $AcWL_5$ is ~17,000 for OBPC, while it is only 7500 for POPC. Second, the entire binding

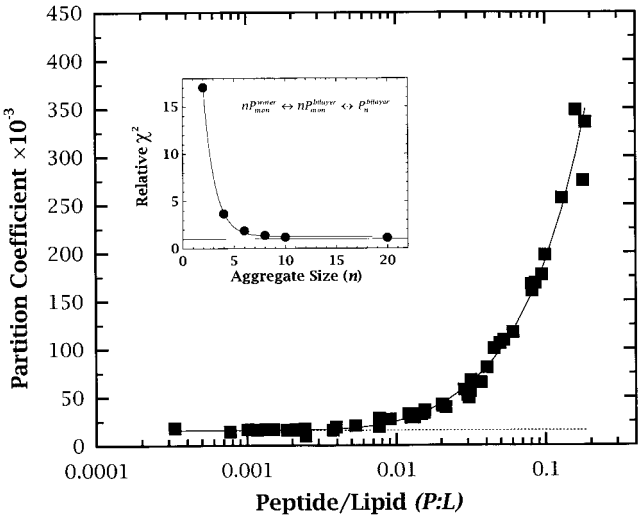

Figure 2. Membrane-concentration dependence of the partitioning of $AcWL_5$ into OBPC vesicles determined using the centrifugation method (see Materials and Methods). Partition coefficients are in mole-fraction units (see Materials and Methods). The peptide per lipid ratio (*P*:*L*) is the ratio of the moles of bound peptide per mole of lipid. The continuous line through the data points is the best-fit of the nucleation-growth model (see Results). The broken line represents the expectation of monomeric partitioning. Inset: The relative χ^2 errors *versus* n for non-linear least-squares curve fitting of the $AcWL_5$ data shown in Figure 2 to a simple monomer–n-mer equilibrium. The χ^2 values are relative to those for the fit of the nucleation-growth model. The inset confirms the results of the nucleation-growth model, that $n \geqslant 10$.

curve is shifted to higher *P:L* values for OBPC compared to POPC. The major, and most important, difference between the curves is that the statistical dispersion of the K_x^a values is much smaller for the OBPC measurements. Thus, the dispersion of the POPC data appears to be related to experimental methodology.

To verify that the aggregation process was truly cooperative, the partitioning data were analyzed using the nucleation/growth model described by Terzi *et al*. (1994a), which assumes a dimeric nucleation step followed by the growth of large aggregates of size *n*. Their model, based on the more general treatment described by Cantor & Schimmel (1980), was derived in the context of the aqueous-phase aggregation of β-amyloid peptide fragment (25-35), but was easily adapted to membrane aggregation by using *P:L* concentration units. Under the assumptions that $n \to \infty$ and $sC_m < 1$, the total concentration of peptide on the membrane C_T is given by:

$$C_T = C_m\left[1 - \sigma + \frac{\sigma}{(1 - sC_m)^2}\right] \quad (1)$$

where C_m is the membrane monomer concentration calculated from the infinite-dilution monomer partition coefficient K_x and the equilibrium peptide concentration in water $[P]_{water}$ using $C_m = K_x[P]_{water}/[W]$. σ is the nucleation parameter and *s* the growth parameter. The apparent partition coefficient K_x^a, which includes both monomers and aggregates, is given by:

$$K_x^a = C_T[W]/[P]_{water} \quad (2)$$

Nucleation/growth models (Cantor & Schimmel, 1980) assume that there will be a distribution of aggregate sizes with mean value:

$$\bar{n} = (1 - sC_m)^{-1} \quad (3)$$

The parameters σ and *s* were determined by iteratively fitting equation (2) to the experimental data using equation (1) for the computation of C_T. The free energy ΔG_{mA} for transferring a monomer into an aggregate was calculated from:

$$\Delta G_{mA} = -RT \ln s \quad (4)$$

and the free energy change per residue from:

$$\Delta G_{residue} = \frac{\Delta G_{mA}}{i} \quad (5)$$

where *i* is the number of residues (six for $AcWL_5$).

The results of the fits of the model to the POPC and OBPC data (Table 2) show that $AcWL_5$ assembles cooperatively ($\sigma \ll 1$) into large aggregates ($\bar{n} > 10$) when partitioned into phosphatidylcholine vesicles. As a check on the reasonableness of aggregates of this size, we also fit the data to a simple monomer–*n*-mer equilibrium model. The inset in Figure 2 shows that the χ^2 values of the fits relative to χ^2 value for the nucleation-growth model are only slightly larger, provided $n \geqslant 10$.

Table 2. Results of fitting of the nucleation-growth model (Terzi *et al*., 1994a) to the partitioning data for POPC and OBPC vesicles shown in Figures 1 and 2, respectively

	POPC	OBPC
Nucleation parameter, σ	0.24 ± 0.10	0.05 ± 0.01
Growth parameter, *s*[a]	563 ± 167	114 ± 10
Aggregate size, $\bar{n}$[b]	11 ± 2	21 ± 1
ΔG_{mA}[c] (kcal mol^{-1})	-3.69 ± 0.21	-2.76 ± 0.05
$\Delta G_{residue}$[d] (kcal mol^{-1})	-0.61 ± 0.04	-0.46 ± 0.01
Monomer K_x[e]	7622 ± 1330	15716 ± 2254
ΔG_m[f] (kcal mol^{-1})	-5.20 ± 0.10	-5.62 ± 0.08

See equations (1) and (2) and the associated text.

[a] Association constants are dimensionless because concentrations on the membrane are in mole fraction units.

[b] Calculated from equation (3).

[c] Calculated from equation (4).

[d] Calculated from equation (5).

[e] Partition coefficient K_x determined for $P:L \leqslant 0.001$ in all cases. K_x for POPC is slightly different from the value in Table 1 because this is a different data set. The two values agree within experimental uncertainty.

[f] $\Delta G_m = -RT \ln K_x$.

Kinetics of $AcWL_5$ aggregation

If the principal cause of cooperative partitioning were aggregation, one would expect the rate of aggregate formation to be slow compared to monomer partitioning. However, the long equilibration times of the equilibrium dialysis and centrifugation measurements precluded direct measurements of partitioning kinetics by those methods. We took advantage of the fact that the intensity of tryptophan fluorescence of both AcWLWLL and $AcWL_5$ increases two- to threefold when they partition into membranes. We therefore examined the time-course of the partitioning of these peptides after the addition of 1 mM POPC LUV to 20 μM or 35 μM peptide solutions. The results are shown in Figure 3. The changes in fluorescence intensity for monomeric AcWLWLL binding to POPC vesicles occur as a single-step process with a half-time of less than 0.2 minute at all peptide concentrations studied. Similar binding half-times have been reported for other monomeric peptides (Schwarz & Beschiaschvili, 1989; Golding *et al*., 1996). The fluorescence changes associated with $AcWL_5$ partitioning, on the other hand, occur as heterogeneous processes that include a small and rapid increase in fluorescence followed by a much larger and slower increase. This is consistent with rapid partitioning of monomers followed by a slower aggregation process that involves recruitment of additional peptide into the membrane. The half-time of the presumed slow-aggregation phase of partitioning is approximately 20 minutes at 35 μM peptide and increases to 35 minutes at 20 μM peptide. The apparent aggregation of $AcWL_5$ in the LUV bilayers is therefore at least two orders of magnitude slower than for the binding of mono-

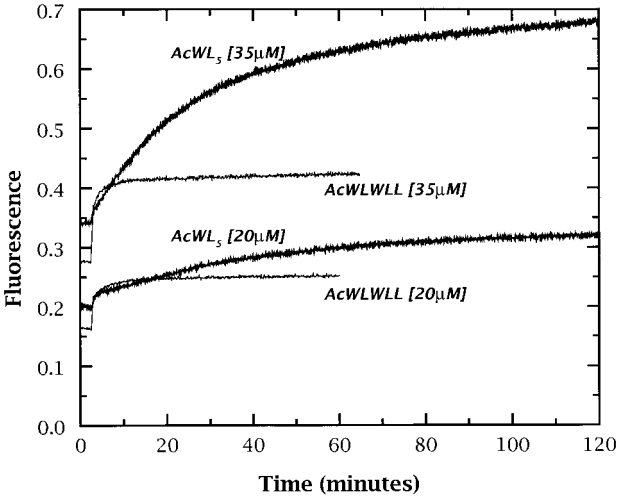

Figure 3. Time dependence of the tryptophan fluorescence of peptides partitioning into POPC vesicles. The partitioning of non-aggregating AcWLWLL quickly reaches a constant plateau level consistent with rapid equilibration of monomers between the water and bilayer phases. The partitioning of aggregate-forming $AcWL_5$ partitions in a biphasic manner that is consistent with initial rapid partitioning of monomers followed by a slower increase due to aggregation of monomers that results in the recruitment of additional peptide into the bilayer. The half-time of the $AcWL_5$ fluorescence increase depends strongly on aqueous peptide concentration, whereas the half-time of AcWLWLL fluorescence does not.

meric peptides, and depends on peptide concentration.

We also assessed dissociation of the $AcWL_5$ from LUV by measuring the rate of digestion by chymotrypsin which, by virtue of its deep catalytic cleft, we expect to act only upon peptides in the aqueous phase. At 0.2 mg/ml chymotrypsin, $AcWL_5$ and AcWLWLL in solution or bound as monomers to membranes are digested with half-times of about one minute. This result supports the idea of rapid equilibration of monomers between the aqueous and bilayer phases. As expected for a slow aggregation process, the digestion of membrane-aggregated $AcWL_5$ proceeded more slowly and in two steps: a fast phase consistent with digestion of monomers, and a slow phase in which 30 to 40% of the total peptide was digested with a half-time of approximately 100 minutes, or about two orders of magnitude more slowly than the digestion of monomers.

These kinetic measurements are entirely consistent with a process involving rapid initial equilibration of $AcWL_5$ monomers into the LUV bilayers followed by a slow aggregation process on the membrane that results in the recruitment of additional monomeric peptide from the aqueous phase. The enzymatic digestion studies suggested that aggregation is reversible. This was confirmed by following the changes in the fluorescence of Trp that occur following additions of peptide-free LUV to previously equilibrated peptide-LUV mixtures. The peptide alone in water exhibits a fluorescence signal typical of water-exposed Trp with the maximum of emission (λ_{max}) located at 350 nm. Addition of 1 mM POPC to a 6 μM peptide solution (low *P*:*L*) results in a moderate blue shift to $\lambda_{max} = 346$ nm, which is the intensity-weighted average of bound and free peptide. Addition of this same amount of lipid to a 40 μM peptide solution (high *P*:*L*) leads to a more pronounced shift to $\lambda_{max} = 340$ nm. A tenfold dilution of this high *P*:*L* sample with a 1 mM peptide-free LUV suspension causes λ_{max} to return to 346 nm. This is consistent with the dilution causing disassembly of the aggregates, desorption of excess monomers into the aqueous phase, and subsequent redistribution of the released peptide to achieve a low *P*:*L* value.

β-Sheet structure of $AcWL_5$ aggregates

We examined the secondary structure of $AcWL_5$ and the control peptide AcWLWLL in buffer, octanol, and POPC LUV using CD spectroscopy. The results for the control peptide are shown in Figure 4A. The variable positive peak at 225 to 230 nm is probably due to the environment-sensitive dichroism of B-band absorbance of the tryptophan residues (Sawyer *et al.*, 1990; Arnold *et al.*, 1992; Woolley & Wallace, 1992; Woody, 1994; Ladokhin *et al.*, 1997a). Nonetheless, all three spectra are practically identical in the more informative region below 225 nm. Specifically, the minima at ~200 nm with intensities of about −20,000 deg $dmol^{-1}$ cm^{-2} are strongly characteristic of random coil peptides (Brahms & Brahms, 1980; Johnson, 1990; Fasman, 1995). We have found that many other small hydrophobic peptides have essentially the same random coil CD spectra in bulk solvents and in membranes (Wimley *et al.*, 1996; Wimley & White, 1996). By the same criteria, $AcWL_5$ also appears to be a random coil in buffer and in octanol (Figure 4B), and in trifluoroethanol (TFE) and sodium dodecyl sulfate (SDS) micelles (data not shown). These results are independent of peptide concentration (Wimley *et al.*, 1996) up to ~0.1 mM. In octanol, we also obtained CD spectra at concentrations between 1 and 50 mM (see Materials and Methods). The mole fraction of peptide is 0.008 at 50 mM peptide, and yet there was no indication of β-sheet structure. The spectra were very similar to those for $AcWL_5$ at low concentration (50 μM, Figure 4B) except that the minimum at ~200 nm was shifted to ~204 nm, and the maximum at 230 nm was somewhat larger.

The structure of $AcWL_5$ in the presence of POPC vesicles is very different. This CD spectrum, measured at a concentration at which most of the $AcWL_5$ will be in the membrane-bound aggregate form, has a minimum at 230 nm that probably arises from the tryptophan, which is known to sometimes have strong negative CD absorbance in this region when bound to membranes in other

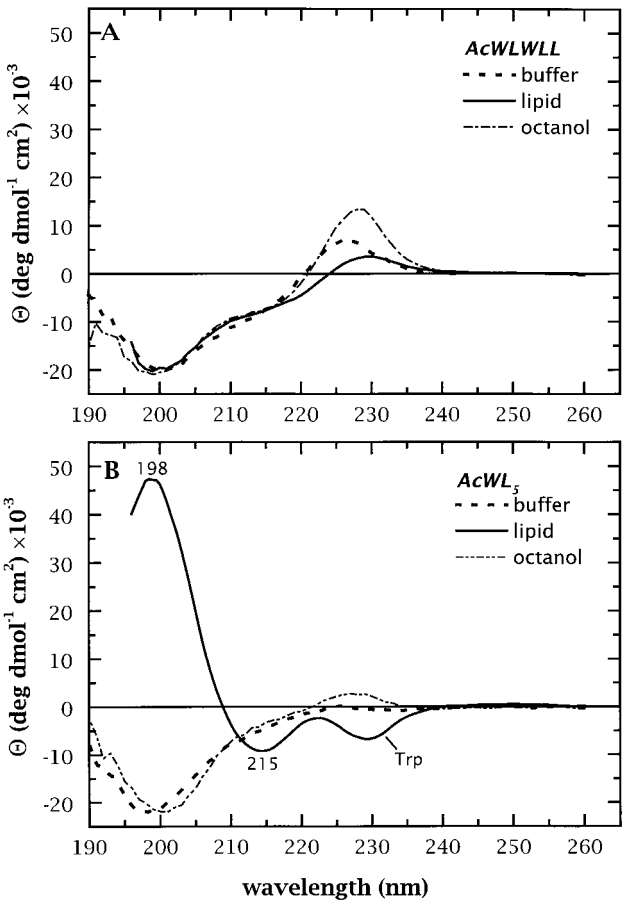

Figure 4. Circular dichroism spectra for $AcWL_5$ and AcWLWLL in buffer, in octanol and in the presence POPC large unilamellar vesicles. Spectra were measured in a 1 mm cuvette containing a 20 to 50 μM peptide solution in 50 mM phosphate buffer, water-saturated octanol, or phosphate buffer containing 1.1 mM POPC vesicles as described in Materials and Methods. The peaks in the vicinity of 230 nm are due to tryptophan. A, Spectra of AcWLWLL. The spectra are consistent with a random-coil conformation of the peptide under all conditions. B, Spectra of $AcWL_5$. The spectra in buffer and octanol are consistent with a random coil structure. But, with peaks at 198 nm and 215 nm, the spectrum for $AcWL_5$ in vesicles is the classical one of antiparallel β-sheet. Therefore, the aggregates of $AcWL_5$ that partition cooperatively into membranes form β-sheet structures.

than α-helical conformations (Woolley *et al.*, 1992; Ladokhin *et al.*, 1997a). The strong maximum at 198 nm and minimum at 215 nm are highly characteristic in both ellipticity and position of classical anti-parallel β-sheet structures (Johnson, 1990; Fasman, 1995; Tilstra & Mattice, 1996). In fact, the CD spectrum of $AcWL_5$ in POPC is very similar below 220 nm to the spectra of OmpA and LamB, well known β-barrel membrane proteins (Fasman, 1995). The CD spectrum of AWL_6 in membranes is very similar to that of $AcWL_5$ and the spectrum of $AcWL_5$ in OBPC is very similar to the spectrum in POPC (data not shown).

Accurate CD spectra for monomeric $AcWL_5$ in membranes are difficult to obtain because there is a lower limit on the peptide concentration (~5 μM) imposed by spectrometer sensitivity, an upper limit on the lipid concentration (~1 mM) imposed by light-scattering artifacts (Glaeser & Jap, 1985), and a reduction in the fraction of $AcWL_5$ bound for lipid concentrations less than 1 mM. Although these limitations make it difficult to separate the contributions of membrane-bound from free monomeric peptide, the CD spectrum of $AcWL_5$ at low concentrations in the presence of membranes does approach that for monomeric random coil peptide in solution. The limited data obtainable thus support the idea that monomeric membrane-bound $AcWL_5$ is a random coil, consistent with our observations on other closely related peptides in the bilayer interface (Wimley & White, 1996).

In order to explore further the structure of $AcWL_5$ in a membrane-like environment, we examined its conformation and orientation in a planar supported DMPC monolayer using PATIR-FTIR spectroscopy (Axelsen *et al.*, 1995a,b). This technique employs a lipid film balance (Langmuir trough) in the course of sample preparation, and provides non-spectroscopic as well as spectroscopic information about the interaction of $AcWL_5$ with a membrane. We observed that the lipid monolayer surface pressure, initially set to 15 dyne/cm, rose upon injection of $AcWL_5$ into the subphase, and reached a plateau at approximately 25 dyne/cm. This did not occur with injections of peptide-free methanol, and thus indicated that $AcWL_5$ partitioned into the monolayer and increased surface pressure until a critical insertion pressure was reached.

The spectroscopic results for the amide I absorption are shown in Figure 5 and summarized in Table 3. The absorption maximum at 1626.7 cm^{-1} is relatively narrow, almost purely Lorentzian in shape, and exhibits a dichroic ratio (R_z) of 1.3. The remaining portions of amide I are well fit by two somewhat broader bands at 1654.3 cm^{-1} ($R_z \approx 2.0$) and 1679.2 cm^{-1} ($R_z \approx 2.5$). Virtually identical results were obtained for $AcWL_6$ (data not shown). This widely split amide I absorption band is characteristic of an anti-parallel β-sheet conformation, with the dominant $\nu_\perp$ (π,0) mode at 1626.7 cm^{-1} oriented perpendicular to the chain axis, and the much weaker $\nu_\parallel$ (0,π) mode at 1679.2 cm^{-1} oriented parallel with the chain axis (Krimm & Bandekar, 1986). The amide I shape is inconsistent with parallel β-sheets (Bandekar & Krimm, 1988a,b), helix, or random coil, all of which should produce a single, unsplit, and relatively broad absorption band. The intermediate component at 1654.3 cm^{-1} most likely has heterogeneous origins, including peptide bonds not involved in secondary structure and the tryptophan side-chain. The acetylated N terminus should not contribute to the band at 1679.2 cm^{-1} because the ^2H_2O-based buffer in the experiments shifts most of the terminus and side-chain assignments

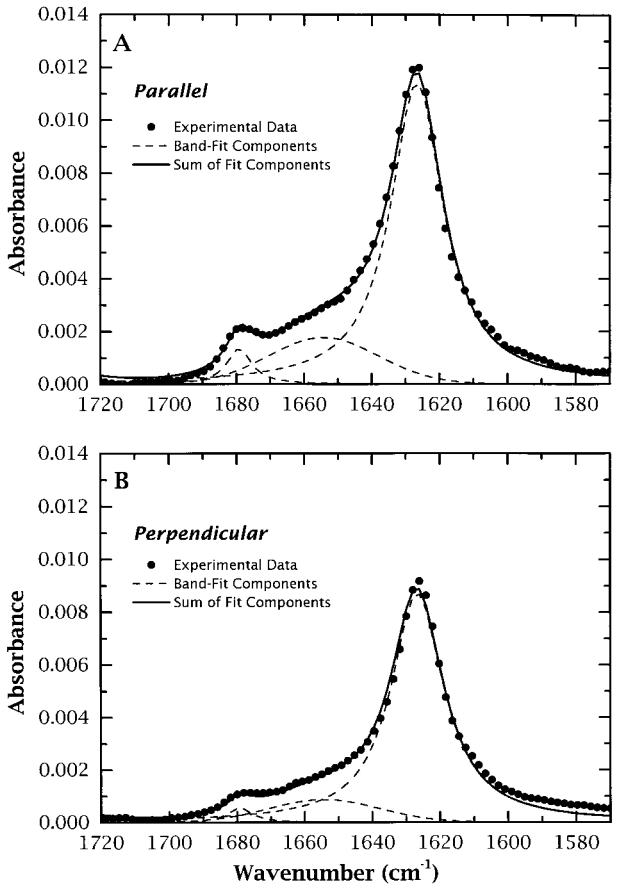

Figure 5. PATIR-FTIR amide I spectra of $AcWL_5$ in a supported DMPC monolayer for the polarizer oriented parallel (A) and perpendicular (B) to the plane of incidence. The spectral data are shown as discrete points, without smoothing, deconvolution or other subjective manipulation. The broken lines indicate the component bands, whose parameters are given in Table 3, while the continuous line is their sum. Spectral features of the lipid monolayer are not seen because they are present in the background spectra that have been subtracted.

made by Venyaminov & Kalnin (1990) to lower frequencies.

As described in detail elsewhere, the isotropic dichroic ratio (R_{iso}) for this system is 2.0 (Citra & Axelsen, 1996; Axelsen & Citra, 1997). The significantly lower ratio of $R_z = 1.3$ for $\nu_\perp$ (π,0) at 1626.7 cm^{-1} indicates that this mode, which is perpendicular to the chain axis, is preferentially aligned parallel with the membrane surface. Because the $\nu_\parallel$ (0,π) mode at 1679.2 cm^{-1} oriented parallel with the chain axis is very weak, there is considerable uncertainty in its R_z of about 2.5; a value of 2.0 cannot be ruled out statistically. The higher value of 2.5 would indicate that the backbone polypeptide chain of $AcWL_5$ is preferentially oriented perpendicular to the membrane surface (Marsh, 1997). In support of the higher value, we note that if there are any terminal, side-chain, or backbone groups not involved in regular secondary structure that contribute to the absorption at 1679.2 cm^{-1}, they are likely to be isotropically oriented. To the extent that their absorption is superimposed on that of the ordered secondary structure, they would tend to cause values of $R_z > 2$ to be underestimated and values of $R_z < 2$ to be overestimated.

Visualizing a pair of antiparallel β-strands as a ladder whose rungs correspond to interstrand hydrogen bonds, the PATIR-FTIR data strongly support a model in which the rungs are parallel with the membrane surface. The ladder can lie flat on the membrane surface, be perpendicular to the surface, or have some intermediate orientation, but cannot lie on its edge with the rungs perpendicular to the surface. If R_z for the $\nu_\parallel$ (0,π) mode at 1679.2 cm^{-1} is 2.5, the perpendicular orientation would be favored. If it is ~2.0, then the angle between the ladder and the surface normal (θ) is not well defined. For $\nu_\parallel$ (0,π) , a value of $R_z = 2.0$ is consistent with a uniform value of $\theta = 54.7°$, a perfectly random distribution of θ, or any distribution for which the mean value of $\cos^2\theta = 1/3$.

Thermal unfolding of membrane aggregates of $AcWL_5$

Taken together, the CD and PATIR-FTIR spectroscopy and the partitioning data show that $AcWL_5$ and related peptides readily assemble into oligomeric β-sheets when bound to membranes. In order to clarify the nature of the assembly process further, we examined the thermal stability of the aggregates through measurements of the CD spectra of $AcWL_5$ in a vesicle solution at temperatures between 5 and 75°C. The concentrations were chosen so that most of the peptide was in the membrane-aggregated form at low temperatures. The results, shown in Figure 6, reveal that the β-sheets in the membrane unfold over the temperature range of 35 to 75°C with a midpoint of approximately 60°C. At the highest temperatures, the peptide appears to be mostly random coil. These temperature-induced changes in CD are rapidly reversible (>one minute) and show no dependence on the thermal history of the samples. Interestingly, the CD spectra of AWL_6 in membranes are very similar to the low-temperature spectra of $AcWL_5$, but are independent of temperature between 5 and 75°C (data not shown). This indicates that the length dependence of the energetics of membrane-induced aggregation of $AcWL_n$ peptides must be very steep, consistent with the observation that $AcWL_4$ does not readily form β-sheets in membranes (Wimley & White, 1996).

The lack of an isodichroic point in Figure 6A indicates the existence of multiple temperature-dependent states and is consistent with a system that is composed of three coupled states: monomers in solution, monomers in the membrane, and aggregates in the membrane. The data suggest that at temperatures greater than ~65°C, the $AcWL_5$ on the membranes is in a predominantly random coil

Table 3. Summary of spectra of the amide I absorption of $AcWL_5$ aggregates adsorbed to a dimyristoylphosphatidylcholine (DMPC) monolayer deposited on germanium measured by PATIR-FTIR

Frequency (cm^{-1})	Amplitudes ∥[c]	⊥[c]	R_z	FWHM[a]	Shape[b]
1626.7	0.01143	0.00872	1.3	18.8	0.0
1654.3	0.00178	0.00087	~2.0	38.2	100.0
1679.2	0.00136	0.00054	~2.5[d]	8.7	68.8

[a] Full-width at half-maximum.
[b] Percentage Gaussian, the remainder is Lorentzian.
[c] ∥ parallel, ⊥ perpendicular.
[d] There is considerable uncertainty in this value. It may be as low as 2.0.

state. That would mean that the partitioning equilibrium should shift towards that for monomeric peptide. We confirmed this by measuring partition coefficients directly at temperatures between 5 and 65°C using equilibrium dialysis. This was done for two samples: one that had low $AcWL_5$ concentration and high lipid concentration (low *P*:*L*), in which the peptide should be predominantly monomeric on the membrane, and one that had high $AcWL_5$ and low lipid (high *P*:*L*) in which the peptide should be predominantly aggregated on the membrane. The temperature dependence of partitioning is weak for monomeric peptides, as demonstrated in Figure 7 by the low *P*:*L* sample of $AcWL_5$ (filled circles) and by AcWLWLL (filled squares). In contrast, the apparent partitioning of $AcWL_5$ at high *P*:*L* (open circles) is very high, but decreases dramatically between 25 and 65°C, which is the same temperature range where the largest changes in CD spectra occur. At 65°C, the

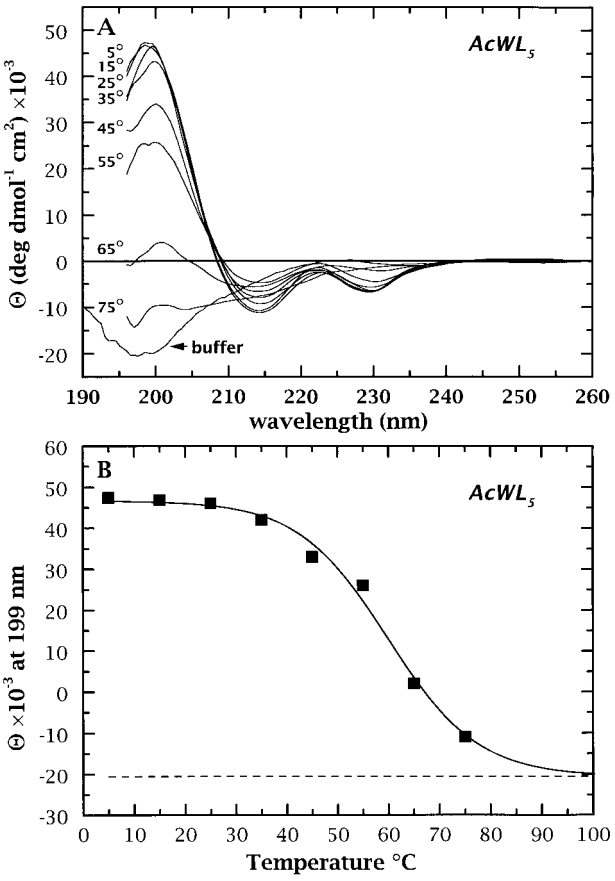

Figure 6. Temperature dependence of the CD spectra of $AcWL_5$ in POPC that demonstrate the thermal unfolding of the β-sheet aggregates. A, CD spectra of 30 μM $AcWL_5$ in the presence of 1.1 mM POPC measured at temperatures between 5 and 75°C. Also shown is the random coil spectrum of $AcWL_5$ in buffer at 25°C. For $AcWL_5$ in POPC, the ellipticity at the characteristic β-structure peak of 199 nm decreases with temperature. At the highest temperature, the spectra approach the random coil spectrum of $AcWL_5$ in buffer. B, Temperature dependence of the molar ellipticity at 199 nm. The reversible changes in the 199 nm ellipticity demonstrate that the β-structure in the membrane unfolds at a temperature of approximately 60°C with a half-width of approximately 20°C. The broken line is the value of ellipticity at 199 nm for $AcWL_5$ in buffer (see A).

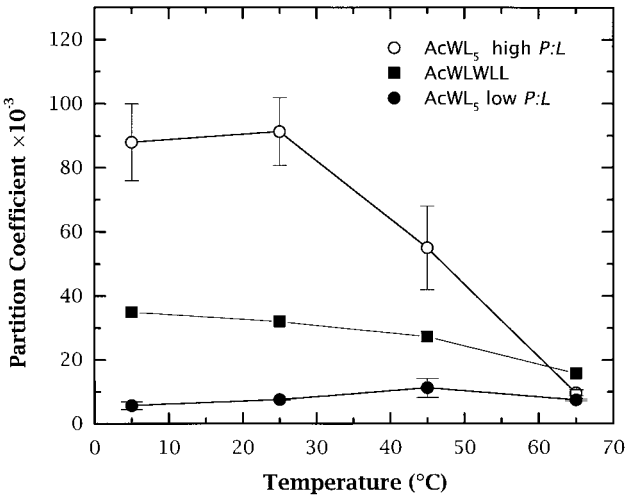

Figure 7. Temperature dependence of the partitioning of AcWLWLL and of $AcWL_5$ at high and low *P*:*L* values. Partitioning was measured using equilibrium dialysis at temperatures between 5 and 65°C. Data for $AcWL_5$ are for a high *P*:*L* (35 μM $AcWL_5$ + 1 mM POPC, open circles), where membrane aggregates will be the dominant form of the bound peptide, and for low *P*:*L* (10 μM $AcWL_5$, 20 mM POPC, filled circles) where monomers prevail. Data for non-aggregating AcWLWLL (filled squares) are shown for comparison. The high degree of partitioning due to aggregation is reversed by high temperature.

partition coefficient, like the CD spectrum, is nearly identical with that for monomeric random coil $AcWL_5$. This is the behavior expected from the three temperature-dependent coupled states proposed earlier. Thus, it appears that the equilibrium between monomers and aggregates on the membrane shifts toward the unfolded monomeric state at high temperatures so that concomitantly the resulting surplus of monomer returns to the aqueous phase. This strengthens the idea that the cooperative binding of $AcWL_5$ and the formation of β-sheet secondary structure are coupled. It also shows that the aggregation state of $AcWL_5$ can be manipulated through changes in temperature, thereby increasing its potential usefulness as a model system.

Effects of $AcWL_5$ on membrane permeability

The permeability of LUV containing $AcWL_5$ aggregates is important for two reasons. First, all of the known β-barrel membrane proteins form pores through membranes that allow the passage of hydrophilic molecules. Although β-barrel pore formation by $AcWL_5$ seemed unlikely because of the bulky hydrophobic side-chains, we nonetheless examined the effects of $AcWL_5$ β-sheets on the permeability of POPC membranes. Second, and more important, the large aggregates might cause a major disruption of vesicle integrity such as lysis or non-vesicular lipid-peptide complexes, and thus weaken the relevance of $AcWL_5$ to the folding of membrane proteins.

Permeability changes were assessed by examining the extent and mechanism of peptide-induced leakage of a fluorescent dye (ANTS) and a quencher (DPX) from POPC LUV using the so-called requenching method in which the dye and quencher are co-encapsulated within vesicles and the extent and mechanism of leakage determined through measurements of ANTS fluorescence. The method has been described in detail elsewhere (Ladokhin *et al.*, 1995, 1997b). Briefly, after incubation with peptide, the level of internal quenching (Q_{in}; 100% quenching corresponds to $Q_{in} = 0$) in a suspension of vesicles containing entrapped ANTS and DPX is measured as a function of the fraction of ANTS that has leaked from the vesicles (f_{out}). The changes in ANTS fluorescence reveal the extent of leakage and the shape of the requenching plot (Q_{in} *versus* f_{out}, Figure 8A) reveals the mechanism. If the leakage is an all-or-none process, the vesicles either leak all of their contents or none, and Q_{in} will always equal the initial value resulting in a horizontal requenching plot (see Figure 8A). All-or-none leakage is generally interpreted to signify either leakage through a large-diameter pore or a large-scale disruption of the membrane, e.g. lysis. If the leakage is graded, then all of the vesicles leak a fraction of their contents and Q_{in} will increase with f_{out}. Graded leakage means that the vesicles remain intact and usually signifies a non-specific disruption of the bilayer permeability barrier. The precise dependence of Q_{in} on f_{out} for graded release depends on the preference for ANTS or DPX release that is described by a parameter α (Ladokhin *et al.*, 1995, 1997b) that has a value of 1 when there is no preference (Figure 8A)

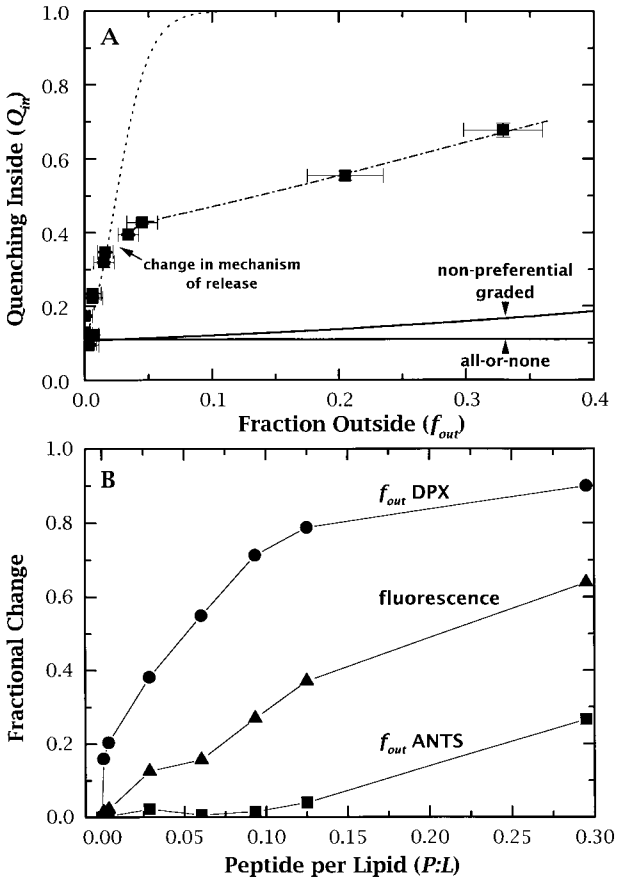

Figure 8. The leakage of vesicle contents induced by $AcWL_5$. Increasing concentrations of $AcWL_5$ were incubated with 0.3 mM POPC preloaded with the anionic fluorescent dye ANTS and the cationic quencher DPX. Leakage was assessed by the requenching method (see Materials and Methods). A, Requenching plot of the internal quenching of the entrapped ANTS by the entrapped DPX as a function of the fraction of ANTS released. The shape of this plot reveals the mechanism of peptide induced leakage. The continuous lines indicate the expectations for all-or-none leakage and non-preferential graded leakage (see Results). For $AcWL_5$, the mechanism of leakage is graded, and at low f_{out} values is almost completely selective for DPX release, giving rise to $\alpha \approx 72$ (dotted curve). At higher values of f_{out}, the selectivity falls to $\alpha \approx 3$ (dot-dash curve), suggesting a change in mechanism of release that could include some lysis. B, The fractional change in fluorescence, due to the $AcWL_5$-induced release of vesicle contents is shown, along with the fractional releases of ANTS and DPX, calculated as described (Ladokhin *et al.*, 1995, 1997b) from the data shown in A. The leakage is graded and, as indicated by the extraordinarily high *P:L* values required, very inefficient. Vesicle integrity must be generally maintained at even the highest *P:L*, otherwise the leakage would be all-or-none.

and a value larger than 1 when DPX leaks preferentially.

The requenching results for $AcWL_5$ are shown in Figure 8. Multiple samples containing the 0.3 mM POPC LUV with entrapped ANTS and DPX were incubated for three hours with increasing amounts of $AcWL_5$. Most important, the requenching experiment shows that leakage is graded rather than all-or-none. This eliminates the possibility of a general large-scale disruption such as lysis. Leakage of DPX is significant only at high peptide concentrations in the bilayer of at least 0.01 peptide molecule per lipid molecule, or ~1000 peptides per vesicle, and leakage of ANTS is significant only if $P{:}L > 0.1$ (Figure 8B). In contrast, some pore-forming peptides induce extensive all-or-none leakage at concentrations as low as 0.0001 peptide/lipid (Parente *et al*., 1990). $AcWL_5$ is thus very inefficient at inducing leakage. In fact, the contents leakage caused by monomeric AcWLWLL is similar (Ladokhin *et al*., 1995). The $AcWL_5$-induced leakage of ANTS and DPX from POPC vesicles is a graded process that is strongly preferential for DPX release, especially at low peptide concentrations (Figure 8A). Selective release of DPX is common in cases of graded release caused by both cationic and anionic peptides (Wimley *et al*., 1994; Ladokhin *et al*., 1995, 1997a; Hristova *et al*., 1996) and indicates a non-specific disruption of the membrane permeability barrier. Only at very high peptide concentrations ($P{:}L > 0.1$) does $AcWL_5$ induce significant leakage of ANTS, suggesting a change in the mechanism of leakage that may include some vesicle lysis (Figure 8A). Nonetheless, we conclude from the ineffective and graded nature of release that $AcWL_5$ assembles into β-sheets in membranes in a manner that causes remarkably small changes in membrane permeability. This is in agreement with the observation that $AcWL_5$ does not increase the Na^+ or K^+ conductance of planar bilayers (Y. Sokolov, J. E. Hall, & W. C. W., unpublished results).

Discussion

$AcWL_5$ exists as a random-coil monomer in the aqueous phase at all concentrations at which it is soluble and in the bilayer phase at low concentrations ($P{:}L < 0.001$). For high membrane concentrations ($P{:}L > 0.001$), it cooperatively assembles into large β-sheet aggregates. The data presented are consistent with the simple equilibrium reaction illustrated in Figure 9. (The structure of the aggregate shown in Figure 9 is for illustrative purposes only and should not be taken literally.) The data in Table 2 indicate that the free energy reduction associated with monomer partitioning is ~5.4 kcal mol^{-1} and that the transfer of a monomer into an aggregate causes an additional reduction of ~3 to 4 kcal mol^{-1}. An important property of $AcWL_5$, emphasized by Figure 9, is that the peptide can enter or leave the bilayer only by monomer partitioning. This is a highly desirable property of future model systems, because it greatly simplifies the interpretation and analysis of the aggregation process.

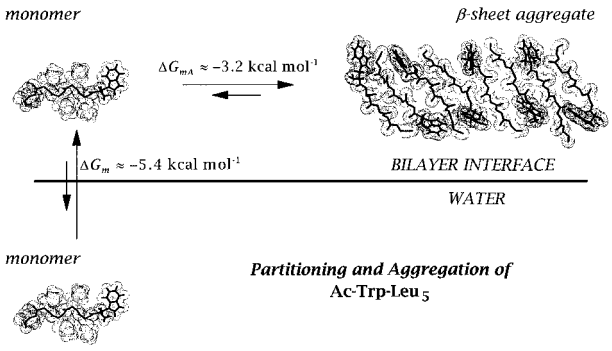

Figure 9. Summary of the partitioning and aggregation of $AcWL_5$ into a POPC or OBPC bilayer interfaces. $AcWL_5$ can enter and leave the membrane only in the monomeric random-coil form. The approximate free energies of transfer shown are averages of the POPC and OBPC values shown in Table 2. The structures of the monomers and aggregate of $AcWL_5$ are shown for illustrative purposes only, and should not be taken literally. Here the aggregate is shown as containing eight monomers; the average aggregate size is actually ten or greater (Table 2). The anti-parallel arrangement of the β-strands shown maximizes the separation between the charged carboxyl-terminal groups (see Discussion).

The detailed structure of the β-sheet aggregates is unknown, but the sequence of $AcWL_5$, our experiments, and the general characteristics of β-sheets, suggest some broad features. First, the average aggregate size is fairly large, 10 to 20 peptides (Table 2), but not huge. Because large aggregates offer the advantage of maximum interstrand hydrogen bonding and consequently maximum reduction in the cost of partitioning peptide bonds, one could imagine a very small number of immensely large aggregates on each vesicle as an extreme possibility. The moderate sizes of the aggregates therefore suggest that interstrand hydrogen bonding is only one of several determinants of aggregate structure. Second, the shape of the amide I absorption band indicates that the β-strands of the aggregates are anti-parallel (Figure 5). They may possibly be staggered (Murzin *et al*., 1994a; Sansom & Kerr, 1995) because the very bulky N-terminal Trp residue and the anionic carboxy terminus would tend to repel nearest neighbors with the same termini. Third, the unequivocal R_z value of 1.3 for the $\nu_\perp$ $(\pi,0)$ mode at 1626.7 cm^{-1} indicates that the interstrand hydrogen bonds are parallel with the membrane surface, while the R_z value of ~2.5 obtained for the $\nu_\parallel$ $(0,\pi)$ mode at 1679.2 cm^{-1} suggests that the β-strands have a perpendicular orientation. However, as noted above, the result for $\nu_\parallel$ $(0,\pi)$ is subject to considerable uncertainty. Fourth, the peptides are probably in the interfacial region of the bilayer because the fluorescence

results show that the intensity change and wavelength shift for $AcWL_5$ aggregates is similar to that for monomeric $AcWL_5$ and AcWLWLL, which are in the bilayer interface (Wimley & White, 1996). Furthermore, deep insertion of the aggregates into the hydrocarbon core is unlikely because the monomers have a pK_a value of 5.7 in the membrane interface (Wimley & White, 1996) so that the carboxyl groups of the aggregates should be fully ionized at pH 7. This was confirmed by the observation that the CD spectrum of $AcWL_5$ in POPC LUV was unchanged at pH 11 (data not shown). At pH 3, the strong minimum in the CD spectrum at 230 nm due to the tryptophan residue was flattened and broadened (data not shown), suggesting a change in the environment of the tryptophan residue due to protonation of the carboxyl groups.

An important characteristic of β-sheets in soluble proteins is their strong tendency to twist and coil (Chothia, 1973, 1984; Richardson, 1981; Chothia, 1984), which can lead to β-barrel structures (Murzin *et al*., 1994a,b). We thus considered, but rejected, the possibility of a β-barrel structure for $AcWL_5$. Examination of β-barrels models by means of molecular graphics indicated that $AcWL_5$ could form barrels with eight or 12 strands with a shear number of 12 (see Murzin *et al*. (1994a) and Sansom & Kerr (1995)). The strands in such barrels would be tilted about 45° with respect to the barrel axis. Regardless of the orientation of the axis with respect to the membrane plane, there would have to be a considerable population of interstrand hydrogen bonds that were not aligned parallel with the membrane plane, which would be inconsistent with the PATIR-FTIR results. Although the β-barrel appears unlikely, we cannot eliminate the possibility that the aggregates form some kind of twisted-sheet structure that is consistent with the PATIR-FTIR results. Simulations *in vacuo* of aggregates of small peptides suggest the feasibility of $AcWL_5$ aggregates forming right-handed twisted sheets (Chou & Scheraga, 1982; Yang & Honig, 1995; Wang *et al*., 1996). However, the relevance of such simulations to peptides in the extremely complex environment of the bilayer interface is problematic. Free energy reductions that favor twisted sheets *in vacuo* could be countered by partitioning issues such as the burial of charges and of peptide bonds in the interface. One can speculate that the balance between these competing requirements may play a role in the determination of aggregate size.

A simple structural arrangement consistent with these various considerations is that the aggregates consist of stacks of small hydrogen-bonded sheets stabilized by the contacts of the Leu side-chains. The stacks would be required to have their hydrogen bonds aligned generally parallel with the membrane surface. Such an arrangement would minimize contacts of the charged carboxyl groups and non-hydrogen-bonded peptide bonds with the surface of the bilayer's hydrocarbon core. Such a stacked arrangement could result in a so-called aligned packing (Chothia, 1984) that could allow staggering as well as some twisting about an axis parallel with the strands while maintaining an H-bond arrangement that is generally parallel with the membrane surface. The fact that Leu, along with Val and Ile, are favored at the interfaces of stacked sheets in proteins (Chothia, 1984) may be significant.

Thermal stability of $AcWL_5$

Membrane proteins have an unusually high thermal stability, which was described by Haltia & Freire (1995) to be the result of the high level of stability of ''intrabilayer secondary structure elements.'' This stability is displayed through the partial unfolding of tertiary structure elements and extrabilayer secondary structure elements but without the complete unfolding of secondary structure elements within the bilayer (Brouillette *et al*., 1987; Haltia & Freire, 1995). The high energetic cost of the open peptide bonds of denatured chains in the membrane is the most likely reason for this effect (Haltia & Freire, 1995). In contrast, the membrane-bound β-sheets of $AcWL_5$ unfold completely and reversibly at a moderate temperature of approximately 65°C, consistent with an interfacial location. The energetic penalty of non-hydrogen bonded peptide bonds is probably smaller in the interface than for membrane protein segments that span the bilayer hydrocarbon core. Perhaps more important is the fact that the unfolded peptides can reduce the cost further by dissociating from the interface into the aqueous phase, an option that is not available to long, hydrophobic transmembrane proteins. This option is also not available to the practically insoluble AWL_6, for example, which may explain the observation that AWL_6 does not unfold at temperatures up to 75°C. The stability of the membrane secondary structure of $AcWL_5$ appears to be exactly poised between the extremes of having no secondary structure as in $AcWL_4$ and secondary structure that is so stable it is difficult to manipulate, as in AWL_6.

The transition half-width of 20°C is surprisingly sharp for a peptide as small as $AcWL_5$. For instance, in the classical Zimm-Doty model of helix-coil transitions (Zimm *et al*., 1959), half-widths become this sharp only when the cooperatively folding chains contain 50 residues or more. Isolated α-helices or small proteins typically have much broader thermal transitions with half-widths of up to 50°C (Merutka & Stellwagen, 1991; Scholtz *et al*., 1991). Transition half-widths as small as that for $AcWL_5$ in membranes occur only for the highly cooperative unfolding of globular proteins, for example, where they typically fall in the range of ~8 to ~20°C (Shortle *et al*., 1988; Pakula & Sauer, 1990; de Francesco *et al*., 1991; Alexander *et al*., 1992; Gittis *et al*., 1993). The relatively sharp transition of $AcWL_5$ is consistent with the involvement of a large number of residues, ≈60 for aggregates with $n = 10$.

The coupling between partitioning and folding of $AcWL_5$ is probably also responsible, in part, for the fact that the cooperativity of its thermal unfolding is nearly as great as for large globular proteins. This is because the monomer-aggregate equilibrium on the membrane is shifted further towards the unfolded state by the dissociation of monomeric peptide into the aqueous phase. In other words, the aqueous phase acts as a sink for monomeric peptide and the favorable dissociation of bound monomers is coupled to unfolding. This amplifies the cooperativity of the thermal unfolding curve (Figure 6).

Energetic considerations of sheet formation in membranes

In water, the hydrogen bonds in a β-sheet define the allowable geometries, but it is uncertain if they contribute favorably to stability. Instead, computer simulations (Chou *et al*., 1982, 1983; Yang & Honig, 1995; Wang *et al*., 1996) have suggested that hydrophobic interactions between non-polar side-chains on adjacent strands probably contribute the dominant stabilizing interactions. This may explain the high sheet-forming propensities of bulky hydrophobic and β-branched amino acids and may also explain, in part, their context dependence (Smith *et al*., 1994; Smith & Regan, 1995). In membranes, the rules governing the energetics of β-sheet formation are likely to be very different. For instance, interactions between non-polar groups will be less potent in bilayers because of the less polar nature of membranes compared to bulk water. Nonetheless, non-polar groups can still make important contributions to peptide interactions in membranes, as demonstrated by structural studies of the transmembrane dimerization of glycophorin A (MacKenzie *et al*., 1997). Also important are the energetic contributions that arise from thermodynamic changes in the bilayer, collectively referred to as bilayer effects (Wimley & White, 1993a; White & Wimley, 1994). The contribution of bilayer effects relative to the contribution of direct interactions between the peptides remains unknown.

Polar interactions, such as hydrogen bonds, are probably more important for driving secondary structure formation in membranes relative to water. We have shown that the free energy cost of moving a non-hydrogen-bonded peptide bond from water into the interface of a membrane is unfavorable by 1.2 kcal mol^{-1} (Wimley & White, 1996). This value might be as high as 3 to 6 kcal mol^{-1} for peptide bonds located deeper in the interior of the membrane (Roseman, 1988; Ben-Tal *et al*., 1996). The simple fact that all transbilayer domains of membrane proteins are either α-helices or β-barrels indicates that peptide bonds involved in hydrogen-bonded secondary structure have a much lower free energy than ''open'' peptide bonds. Thus, even for small peptides like $AcWL_5$ located in membrane interfaces, hydrogen bonding should have a much more favorable effect on free energy than in water. In fact, we show in Table 2 that the experimentally observed effects can be accounted for by net free energies reductions of 0.46 to 0.61 kcal mol^{-1} per residue. This modest per-residue reduction can lead to an enormous total free energy reduction for the folding of, say, the β-barrel pore of α-hemolysin. With approximately 100 residues comprising the transmembrane portion of the pore, the free-energy reduction driving assembly of the pore could be ~50 kcal/mol. The actual total free energy reduction is no doubt much smaller. A more reasonable value of ~10 kcal/mol would require only 0.1 kcal/mol reduction per residue, which the work presented here shows to be quite feasible.

The hydrogen-bond effect helps explain the facile formation of peptide secondary structure in membranes in general (Kaiser & Kezdy, 1983), and in particular from a peptide as small as $AcWL_5$ bound at the membrane interface. However, one cannot necessarily assume that the hydrogen-bond effect is the sole contributor to the free energy reduction or that it is simple. This is shown, for example, by the fact that AcWLWLL does not form β-sheets in membranes at concentrations at which $AcWL_5$ readily does so. Other contributions that are expected to favor the formation of sheets include side-chain-specific effects (Li & Deber, 1994; Deber & Li, 1995) and the entropic advantage gained from the high concentration of peptide achievable in the interface compared to a bulk phase. A comparison of the data for OBPC and POPC of Table 2 shows that there are lipid-dependent subtleties as well: All of the parameters for $AcWL_5$ partitioning and aggregation are statistically different, and in surprising ways. For example, even though the partition coefficient for OBPC is about the twice the value for POPC, the onset of aggregation occurs at a higher *P*:*L* value than for POPC. Interestingly, the partition coefficient of AcWLWLL is exactly the same for POPC and OBPC vesicles. These and the other differences may be due to slight differences in the area/lipid and/or the presence of the bromines in OBPC. In any case, the hydrogen-bond effect is likely to depend strongly on the structure of the lipid, especially the headgroup, and other presently unknown details of peptide-bilayer interactions.

The rules governing the energetics of secondary structure formation in membranes and in water are different, as shown by Deber and colleagues (Li & Deber, 1994; Deber & Li, 1995). For example, they have found that the bulky, hydrophobic residues that are good β-sheet formers (poor helix formers) in water are very good helix-formers in membranes. Leucine, however, is a good helix former in water (O'Neil & DeGrado, 1990) as well as membranes. Why then do $AcWL_5$ and $AcWL_6$ form β-sheets? Part of the answer may be that, as helices, the peptides would always have the equivalent of about four open peptide bonds at the helix ends. In a large stacked β-sheet arrangement, the number of open peptide bonds per peptide would be con-

siderably smaller. At what length might these types of peptides adopt a helix rather than a sheet structure in membranes? The leucine-based peptides $K_2GL_mK_2A$-amide with $m = 16$ or 24 are known to form transmembrane α-helices (Davis *et al.*, 1983; Huschilt *et al.*, 1989). We have found that $AcWL_n$ peptides as long as nine residues form β-sheets in POPC bilayers, suggesting that the critical number of leucine residues for helix formation is between ten and 16.

$AcWL_5$ as a peptide model system

There are a few examples of peptides as small as ten to 16 residues that form β-sheets in water (Lang *et al.*, 1992; Terzi *et al.*, 1994a; Forood *et al.*, 1995; Zhang & Rich, 1997), and peptides as small as tripeptides, including tri-L-leucine (Go & Parthasarathy, 1995), that form β-sheets in crystals, but the easy formation of β-sheets from low concentrations of the anionic hexapeptide $AcWL_5$ in membranes is unexpected. This is especially true because, unlike most other peptides that gain secondary structure in membranes, $AcWL_5$ does not partition exceptionally strongly, probably does not penetrate the membrane hydrocarbon layer to a large extent, and is not amphipathic. There are, of course, other peptides unrelated to the $AcWL_n$ that have been shown to form β-sheets on membranes (Krantz *et al.*, 1991; Terzi *et al.*, 1994b; Lee *et al.*, 1995; Mancheño *et al.*, 1995; Aggeli *et al.*, 1996) in addition to the β-barrel membrane proteins and protein toxins mentioned earlier. For example, a synthetic 24-residue peptide analog of a leucine-rich repeat motif (Krantz *et al.*, 1991) was shown by circular dichroism to have significant β-sheet content in solution, but even more on membranes. This peptide also forms channels in planar bilayers and was shown by freeze-fracture electron microscopy to form 60 Å intramembranous particles, suggesting transmembrane peptide aggregates. Also the peptides benzyl-L-$(Leu)_n$-*O*-ethyl ($n = 5$, 6 or 7) were shown to have circular dichroism spectra in membranes that are consistent with a complex mixture of α-helix, β-sheet and random coil secondary structure (Lee *et al.*, 1995). Finally, several signal peptides (Cornell *et al.*, 1989; Tamm, 1991) and several cationic fragments of the β-amyloid protein have enhanced β-structure in the presence of anionic membranes (Terzi *et al.*, 1994b, 1995) or lipid micelles (Fletcher & Keire, 1997).

These examples notwithstanding, the thermodynamic principles of β-sheet formation on membranes are virtually unexplored. For this reason, the study of $AcWL_5$ and related peptides provides a good beginning. This is true, in part, because the assembly of $AcWL_5$ in membranes occurs in a manner that can be manipulated, for example, by changing the system temperature or the concentration of peptide and lipid. Furthermore, they preserve some of the fundamental features of β-barrel membrane protein assembly. Like α-hemolysin, for example, $AcWL_5$ is reasonably soluble in water but also binds to membranes and assembles into multimeric β-sheets there. We do not know if the formation of β-sheets in membranes is a general property of small hydrophobic peptides in the bilayer interface or if it is a fortuitous consequence of the primary structure of $AcWL_5$ and AWL_6. We do know that AcWLWLL does not form β-sheets at any concentration that we have examined, and that it does not interact with $AcWL_5$ β-sheets even when both are present in the same membrane (see Table 1). This is despite the fact that both are very similar in sequence and size and AcWLWLL is more hydrophobic than $AcWL_5$. $AcWL_5$ and AWL_6 thus provide a useful starting point for clarifying fundamental issues and subsequently for engineering the next generation of peptide model systems for β-sheet formation in membranes.

Materials and Methods

Materials

Synthesis and purification of peptides have already been described in detail (Wimley *et al.*, 1996). The identity of all peptides was confirmed with fast-atom bombardment mass spectrometry, and all were at least 99.5% pure. Peptide solutions in buffer were prepared by evaporating the methanol from an aliquot of a stock methanol solution in a vial followed by the addition of buffer. Solutions close to the solubility limit of the peptides were warmed and sonicated, and then filtered or centrifuged before use. Peptide + lipid solutions were made either by adding a concentrated lipid solution to an aqueous solution of peptide or *vice versa*. The manner of preparation had no appreciable effect on the results. Except where noted, the buffer used was 10 mM Hepes (pH 7.0), 50 mM KCl, 1 mM EDTA, 3 mM NaN_3. Measurements made at pH 11 were identical with those made at pH 7, indicating that the carboxy terminus is fully ionized in our experiments. This is consistent with the fact that the pK_a of the carboxyl group shifts from 3.7 in water to 5.7 in membranes (Wimley & White, 1996). DOPC, OBPC and perdeuterated DMPC were purchased from Avanti Polar Lipids (Alabaster, AL). The purity of OBPC was determined by elemental analysis to be > 99.9% (Microlit Laboratories, Madison, NJ).

Peptide solubility

The aqueous phase solubility of $AcWL_5$ and AWL_6 were measured in a solution that was prepared in the following manner: buffer was added to a vial containing an excess of lyophilized peptide, which was then warmed to 50°C and bath sonicated for ten minutes. After cooling the vial to room temperature for one hour, the sample was filtered through an 0.22 μM nylon filter, and the peptide remaining in the filtrate was assayed by HPLC. As we have shown (White *et al.*, 1997), the solubility is a very steep function of peptide length for the $AcWL_n$ series and is equal to ~1 mM for $AcWL_4$, ~0.05 mM for $AcWL_5$, and ~0.0006 mM for AWL_6. The saturated solution of $AcWL_5$ produced in this manner is a monomeric random coil as determined by circular dichroism spectroscopy, fluorescence spectroscopy, fluorescence quenching, and titration calorimetry (Wimley *et al.*, 1996).

Partition coefficient measurements

Partition coefficients for POPC vesicles were determined using equilibrium dialysis and quantitative reverse-phase HPLC as described (Wimley & White, 1993b, 1996; White *et al*., 1997). Briefly, lipid and peptide solutions were placed in opposing 1 ml equilibrium-dialysis half-cells separated by a Spectrapor 2 dialysis membrane (Spectrum Medical, Los Angeles). The cells were rotated at 20 rpm in a temperature-controlled water bath. Equilibration of peptide between the two half-cells, in the absence of lipid, occurred in approximately five hours. The filled dialysis cells were allowed to equilibrate for 24 hours before the concentrations of peptide in the two half-cells were measured by HPLC (Wimley & White, 1993b). No change in apparent partitioning occurred after 24 hours. To high accuracy (White *et al*., 1997; Ladokhin *et al*., 1997a), mole-fraction partition coefficients were computed using:

$$K_x^a = \frac{[P]_{bilayer}/[L]}{[P]_{water}/[W]} \quad (6)$$

where [P] is the peptide concentration in the bilayer or water phase, [L] is the molar lipid concentration, and [W] is the water molar concentration (55.3 M at 25°C). Lipid concentrations varied between 0.3 and 20 mM, and peptide concentrations varied between 5 and 70 μM.

For OBPC vesicles, partition coefficients were determined by a centrifugation method (White *et al*., 1997). The lipid and peptide were mixed in a microcentrifuge vial and incubated overnight. Total peptide in the solution was assayed by quantitative reverse-phase HPLC before centrifugation, and unbound peptide was assayed in the supernatant after progressive centrifugation of the vesicles for 30 minutes each at 4500, 9000 and 16,000 *g* in a Biofuge A centrifuge (Heraeus-Christ GmbH, Osterode, Germany). Under these conditions, the fraction of OBPC in the supernatant was less than 5%. The progressive centrifugation was necessary because we have found that the measured partition coefficients depend on lipid concentration and centrifugation speed if samples with low lipid concentration were centrifuged at high speed (White *et al*., 1997). There is no such dependency for samples centrifuged using the progressive increases in speed listed above. Because $[P]_{total} = [P]_{water} + [P]_{bilayer}$, the partition coefficient may be calculated from equation (6), which becomes:

$$K_x^a = \frac{([P]_{total} - [P]_{water})/[L]}{[P]_{water}/[W]} \quad (7)$$

The total peptide concentration was varied between 5 and 180 μM, and the lipid concentration between 0.5 and 10 mM. The concentration of free peptide was never more than 40 μM, which is below the solubility limit of $AcWL_5$ in buffer.

Fractional partitioning of peptides

Neither AcWLWLL nor $AcWL_5$ partition into membranes so strongly that they will be completely bound under most experimental conditions. The fraction of peptide bound was calculated using:

$$f_b = \frac{K_x^a[L]}{K_x^a[L] + [W]} \quad (8)$$

where K_x^a is the apparent mole-fraction partition coefficient, shown in Figures 1 and 2. In the circular dichroism and fluorescence experiments, we used 1.0 or 1.1 mM POPC LUV, corresponding to $f_b = 0.35$ for AcWLWLL. Consequently, the spectroscopic results are a weighted average of bound and unbound forms. Although, in principle, one can extract the contribution of the membrane-bound form, we chose not to do so in these experiments. For $AcWL_5$, the fraction bound is less precisely known because of the higher uncertainty in the partition coefficients for POPC (see Results). However, it is between 60 and 75% under the conditions of the CD or fluorescence experiments.

Circular dichroism

Circular dichroism measurements were performed using a Jasco J720 CD spectrometer (Japan Spectroscopic Co., Ltd., Tokyo). Phosphate buffer (50 mM KPO_4, pH 7) was used in most experiments because it lacks the strong near-UV absorbance of the Hepes buffer. We determined by means of equilibrium dialysis, circular dichroism, and fluorescence that the binding and aggregation of $AcWL_5$ are very similar in the two buffers. Peptide concentrations were between 5 and 100 μM. Most lipid-containing samples had a concentration of 1.1 mM lipid in the form of POPC LUV. Samples were placed in a 1 mm quartz cuvette and at least 20 scans were collected and averaged. Scanning rate was 20 nm/minute, slits were set to 1 nm, and the response time was two seconds. Proper calibration was confirmed routinely through the use of a 1-camphor, 3 sulfonic acid (CSA) standard solution of known molarity. The possible effects of lipid scattering artifacts were assessed by measuring the CD spectra in the presence and absence of lipid of (1) CSA and (2) a low-binding random coil peptide, AcWLDLL (Wimley & White, 1996). In both cases, the apparent ellipticity was unaffected by 1.1 mM lipid at wavelengths above approximately 197 nm, but was strongly attenuated below that wavelength.

Samples of $AcWL_5$ in POPC vesicles were prepared for CD by any of the following three methods: addition of lipid to $AcWL_5$ dissolved in buffer; addition of a concentrated methanol solution of $AcWL_5$ to lipid in buffer; or addition of lipid in buffer to a vial containing dry $AcWL_5$. The first two methods reproducibly gave the same results as did the third, provided that the sample was warmed, sonicated, or shaken to ensure that all of the dried peptide was dissolved. In this case, warming the sample to 65°C followed by ten minutes of mixing was generally sufficient to fully dissolve the peptide. Complete solution was assured by comparing the expected and measured peptide concentrations, and by the failure of centrifugation to remove peptide from solution. For the insoluble peptides $AcWL_6$, $AcWL_7$, and $AcWL_8$, we found that only the addition of a concentrated methanol solution to lipid in buffer followed by at least one hour of mixing gave reproducible results; and only by this method did the peptide come to exist in a ''soluble'' form (probably membrane-bound aggregates) such that it could not be removed from the solution by centrifugation. We assume that this soluble peptide is partitioned into the vesicles, because the peptide precipitate that forms in the absence of lipid is completely removed by centrifugation or by ultrafiltration.

Measurements on peptides dissolved in octanol at 1 to 50 mM concentrations were performed by placing 1 to 5 μl of concentrated solution between flat quartz disks. The peptide was dried onto one disk within a 5 mm spot and was then dissolved in 1 to 5 μl of octanol while stir-

ring with a syringe tip. The peptide dissolved readily at concentrations up to 50 mM. A second quartz disk was placed on the first, which caused the sample to spread over the 2.19 cm^2 interface between the disks. Pathlengths were calculated from the contact area and the volume of octanol used.

PATIR-FTIR spectroscopy

Polarized attenuated total internal reflection Fourier transform infrared (PATIR-FTIR) spectroscopy was performed using a BioRad FTS-60A spectrometer equipped with an MCT detector and coupled to a lipid film balance. The instrument is configured as described in detail elsewhere (Axelsen *et al*., 1995a,b) except that the internal reflection element is now a 50 mm × 10 mm × 2 mm silanized germanium crystal trapezoid with 45° end-facets, which is applied flat onto the monolayer surface. The subphase volume is approximately 5 ml, and the crystal covers approximately one-third of the subphase surface.

The subphase buffer was 30 mM Hepes in ^2H_2O (pD 7.1), filtered through an 0.2 μm membrane, and cleaned by compression of the surface and aspiration of particulate matter until a surface tension of ~72 dyne/cm was achieved. Perdeuterated DMPC was applied to the subphase surface in a few microliters of 90% hexane, 10% ethanol, and allowed to spread for 30 minutes in a ^2H_2O-saturated argon atmosphere at 25°C. Following this, the monolayer was compressed to a surface pressure of 15 dyne/cm over 15 minutes, and then allowed to equilibrate for another 15 minutes.

At this point, the internal reflection element was slowly lowered onto the subphase surface, and background single-beam spectra were collected with a polarizer oriented parallel with and perpendicular to the plane in which the spectrometer beam is incident on the crystal surface. All spectra (background and sample) are derived from 256 co-added interferograms with triangular apodization and one level of zero filling.

Peptides were dissolved in deuterated methanol and introduced through the monolayer and into the magnetically stirred buffer subphase using a Hamilton microliter syringe and needle. Injection volumes ranged from 18 to 40 μl, yielding a final methanol concentration of less than 1%. An absorbance band due to methanol at 1015 cm^{-1} is observed immediately following the injection of sample, but its intensity declined to 20% of its original height by 30 minutes. The height of the amide I absorbance band due to peptide rose gradually but tended to plateau within ten to 15 minutes, such that spectra collected at 30 and 60 minutes were virtually identical.

Samples of $AcWL_4$, $AcWL_5$ and $AcWL_6$ were examined at subphase concentrations of approximately 700, 20 and 3 μM, respectively, in a subphase volume of approximately 5 ml. After 60 minutes, $AcWL_4$ yielded a barely detectable signal at 1630 to 1640 cm^{-1} and thus could not be studied quantitatively. In contrast, $AcWL_6$ yielded clearer spectra due to its much greater tendency to partition into the membrane. $AcWL_5$, with a partitioning behavior intermediate between that of $AcWL_4$ and $AcWL_6$, yielded results that were frequently not suitable for complete quantitative analysis. The chief difficulty is stability of the instrument and experimental conditions for the 20 to 30 minutes interval between collection of background and sample spectra. For $AcWL_5$, it was exceedingly difficult to obtain a sufficiently high signal-to-noise ratio to permit quantitative analysis. Nevertheless, in all five trials with $AcWL_5$ a dichroic ratio of 1.3(±0.1) was obtained for the 1626.7 cm^{-1} absorption band. In contrast, quantitative analysis of the 1679.2 cm^{-1} band for was possible in only one of the five trials.

The paired spectra (parallel and perpendicular) were analyzed using software (Irfit) written by one of us (P.H.A.) for interactive ''linked'' analysis. This software fits any individual spectrum with an arbitrary number of component bands, each of which is described by a frequency centroid, as well as amplitude, width and shape (Gaussian *versus*. Lorentzian) parameters. In addition, there is a single, straight and level baseline offset parameter. The program seeks a minimum least-squares residual difference between the fit and the data using a downhill simplex algorithm (Press *et al*., 1989). It terminates when the same solution is returned in spite of a 10% perturbation of height, width, shape or baseline parameters, and a 0.1% perturbation of the frequency parameter. In a typical application, as performed in this case, pairs of corresponding spectra are fit simultaneously with the same number of component bands, and all of the parameters for each band, except for amplitudes and baseline offsets, are constrained to be identical for both spectra (i.e. they are linked). For polarized spectra, this approach embodies the assumption that two spectra that differ only in their polarization should be comprised of component bands that differ only in their relative amplitudes. This analytic approach dramatically reduces the ratio of fitting parameters to data, which is a key advantage of the so-called global analysis approach to fluorescence lifetime analysis (Knutson *et al*., 1983). The program structure of Irfit was derived directly from the program Efit, written earlier by one of us (P.H.A.) for fluorescence lifetime analysis (Axelsen *et al*., 1991).

When all parameters describing a component band apart from its amplitude are constrained to be identical in two different spectra, the dichroic ratio (R_z) for that component is simply the ratio of the parallel/perpendicular amplitudes (i.e. it is not necessary to calculate a band area). The dichroic ratios obtained in this manner are compared to an isotropic ratio (R_{iso}) indicating whether the vibrational transition moment for the mode giving rise to that component is preferentially oriented perpendicular to ($R_z > R_{iso}$) or parallel with ($R_z < R_{iso}$) the surface of the internal reflection element surface that supports the membrane. For this system, we employ the ''two-phase'' approximation (Citra & Axelsen, 1996), which yields $R_{iso} = 2.0$ for any internally reflecting interface for which the incidence angle is 45°.

Fluorescence spectroscopy

Fluorescence spectroscopy was performed with an SLM-Aminco (Rochester, NY) 84000 steady-state fluorescence spectrometer. Excitation was set to 260 nm, emission to 340 nm, and slits to 4 nm. In all cases, the magic-angle setting of the polarizers (ex 54.7°, em 0°) were used to reduce artifacts that could arise from light-scattering and to eliminate instrumental sensitivity to tryptophan polarization. The direct contribution of light-scattering was negligible and the attenuation of tryptophan fluorescence at these lipid concentrations due to scattering was less than 5%. The tryptophan fluorescence of bound AcWLWLL and $AcWL_5$ is shifted to lower wavelengths and increases in intensity by about three-

fold compared to the fluorescence of the peptides in solution. For the kinetic experiments, an aliquot of concentrated lipid solution was added to the peptide solution and intensity changes monitored for two hours, and the time for 50% of the total change subsequently determined.

Chymotrypsin digestion

Peptide or peptide + lipid were dissolved in buffer and allowed to equilibrate. Digestion with chymotrypsin was initiated by adding 10% (v/v) of a 2 mg/ml solution of chymotrypsin. The fraction of undigested peptide was monitored by quantitative reverse-phase HPLC (Wimley & White, 1993b). The inherent activity of 0.2 mg/ml chymotrypsin solution was unchanged over the two hours course of the experiments.

Leakage of ANTS and DPX

Leakage of the cationic fluorescent dye ANTS and its obligate anionic quencher DPX were used to assess the effects of $AcWL_5$ on membrane integrity. The determination of the extent and mechanism of peptide-induced leakage has been described in detail elsewhere (Ladokhin *et al*., 1995, 1997b). Briefly, a 100 mM solution of POPC LUV was prepared in the presence of 10 mM each ANTS and DPX. This solution was eluted over a 1 cm × 25 cm gel-filtration column packed with Sephadex G-100 (Sigma Chemical Co., St. Louis, MO). The vesicles with entrapped ANTS and DPX, which eluted in the void volume, were free from external ANTS and DPX. These vesicles were diluted to 0.3 mM and used immediately in the leakage experiments.

Acknowledgments

The research was supported in part by grants from the National Institutes of Health, GM-46823 (to S.H.W.), AI-31696 and AI-22931 (to Michael E. Selsted), and GM54617 (to P.H.A.) and by a grant-in-aid to P.H.A. from the American Heart Association, SE Pennsylvania Affiliate. We thank Dr Mark Sansom for providing the coordinates of alanine β-barrel models.

References

Aggeli, A., Boden, N., Cheng, Y.-L., Findlay, J. B. C., Knowles, P. F., Kovatchev, P., Turnbull, P. J. H. & Marsh, D. (1996). Peptides modeled on the transmembrane region of the slow voltage-gated IsK potassium channel: structural characterization of peptide assemblies in the β-strand conformation. *Biochemistry*, **35**, 16213–16221.

Alexander, P., Fahnestock, S., Lee, T., Orban, J. & Bryan, P. (1992). Thermodynamic analysis of the folding of the streptococcal protein-G IgG-binding domains B1 and B2: why small proteins tend to have high denaturation temperatures. *Biochemistry,* **31**, 3597–3603.

Arnold, G. E., Day, L. A. & Dunker, A. K. (1992). Tryptophan contributions to the unusual circular dichroism of fd bacteriophage. *Biochemistry,* **31**, 7948–7956.

Axelsen, P. H. & Citra, M. J. (1997). Orientational order determination by internal reflection infrared spectroscopy. *Prog. Biophys. Mol. Biol.* **66**, 227–253.

Axelsen, P. H., Bajzer, Z., Prendergast, F. G., Cottam, P. & Ho, C. (1991). Resolution of fluorescence intensity decays of the two tryptophans in glutamine-binding protein of *E. coli* using tryptophan mutants. *Biophys. J.* **60**, 650–659.

Axelsen, P. H., Braddock, W. D., Brockman, H. L., Jones, C. M., Dluhy, R. A., Kaufman, B. K. & Puga, F. J., II (1995a). Use of internal reflectance infrared spectroscopy for the *in situ* study of supported lipid monolayers. *Appl. Spectrosc.* **49**, 526–531.

Axelsen, P. H., Kaufman, B. K., McElhaney, R. N. & Lewis, R. N. A. H. (1995b). The infrared dichroism of transmembrane helical polypeptides. *Biophys. J.* **69**, 2770–2781.

Bandekar, J. & Krimm, S. (1988a). Normal mode spectrum of the parallel-chain β-sheet. *Biopolymers,* **27**, 909–921.

Bandekar, J. & Krimm, S. (1988b). Vibrational spectroscopy of L-valyl-glycyl-glycine, a parallel-chain β-structure. *Biopolymers,* **27**, 885–908.

Ben-Tal, N., Ben-Shaul, A., Nicholls, A. & Honig, B. (1996). Free-energy determinants of α-helix insertion into lipid bilayers. *Biophys. J.* **70**, 1803–1812.

Brahms, S. & Brahms, J. (1980). Determination of protein secondary structure in solution by vacuum ultraviolet circular dichroism. *J. Mol. Biol.* **138**, 149–178.

Brouillette, C. G., Muccio, D. D. & Finney, T. K. (1987). pH dependence of bacteriorhodopsin thermal unfolding. *Biochemistry,* **26**, 7431–7438.

Cantor, C. R. & Schimmel, P. R. (1980). *Biophysical Chemistry,* W. H. Freeman, San Francisco.

Chothia, C. (1973). Conformation of twisted β-pleated sheets in proteins. *J. Mol. Biol.* **75**, 295–302.

Chothia, C. (1984). Principles that determine the structure of proteins. *Annu. Rev. Biochem.* **53**, 537–572.

Chou, K.-C. & Scheraga, H. (1982). Origin of the right-handed twist of β-sheets of poly(L-Val) chains. *Proc. Natl Acad. Sci. USA,* **79**, 7047–7051.

Chou, K.-C., Pottle, M., Némethy, G., Ueda, Y. & Scheraga, H. A. (1982). Structure of β-sheets. Origin of the right-handed twist and of the increased stability of antiparallel over parallel sheets. *J. Mol. Biol.* **162**, 113–130.

Chou, K.-C., Némethy, G. & Scheraga, H. (1983). Role of interchain interactions in the stabilization of the right-handed twist of β-sheets. *J. Mol. Biol.* **168**, 389–407.

Citra, M. J. & Axelsen, P. H. (1996). Determination of molecular order in supported lipid membranes by internal reflection Fourier transform infrared spectroscopy. *Biophys. J.* **71**, 1796–1805.

Cornell, D. G., Dluhy, R. A., Briggs, M. S., McKnight, C. J. & Gierasch, L. M. (1989). Conformations and orientations of signal peptide interacting with phospholipid monolayers. *Biochemistry,* **28**, 2789–2797.

Cornut, I., Büttner, K., Dasseux, J.-L. & Dufourcq, J. (1994). The amphipathic α-helix concept: application to the *de novo* design of ideally amphipathic Leu, Lys peptides with hemolytic activity higher than that of melittin. *FEBS Letters,* **349**, 29–33.

Dathe, M., Schümann, M., Wieprecht, T., Winkler, A., Beyermann, M., Krause, E., Matsuzaki, K., Murase, O. & Bienert, M. (1996). Peptide helicity and membrane surface charge modulate the balance of electrostatic and hydrophobic interactions with lipid bilayers and biological membranes. *Biochemistry,* **35**, 12612–12622.

Davis, J. H., Clare, D. M., Hodges, R. S. & Bloom, M. (1983). Interaction of a synthetic amphiphilic poly-

peptide and lipids in a bilayer structure. *Biochemistry,* **22**, 5298–5305.

Deber, C. M. & Li, S.-C. (1995). Peptides in membranes: helicity and hydrophobicity. *Biopolymers,* **37**, 295–318.

de Francesco, R., Pastore, A., Vecchio, G. & Cortese, R. (1991). Circular dichroism study on the conformational stablility of the dimerization domain of transcription factor LFB1. *Biochemistry,* **30**, 143–147.

Do, H., Falcone, D., Lin, J., Andrews, D. W. & Johnson, A. E. (1996). The cotranslational integration of membrane proteins into the phospholipid bilayer is a multistep process. *Cell,* **85**, 369–378.

Dornmair, K., Kiefer, H. & Jähnig, F. (1990). Refolding of an integral membrane protein: OmpA of *Escherichia coli*. *J. Biol. Chem.* **265**, 18907–18911.

Eisele, J. L. & Rosenbusch, J. P. (1990). *In vitro* folding and oligomerization of a membrane protein: transition of bacterial porin from random coil to native conformation. *J. Biol. Chem.* **265**, 10217–10220.

Fasman, G. D. (1995). The measurement of transmembrane helices by the deconvolution of CD spectra of membrane proteins: a review. *Biopolymers,* **37**, 339–362.

Fletcher, T. G. & Keire, D. A. (1997). The interaction of β-amyloid protein fragment (12-28) with lipid environments. *Protein Sci.* **6**, 666–675.

Forood, B., Pérez-Payá, E., Houghten, R. A. & Blondelle, S. E. (1995). Formation of an extremely stable polyalanine β-sheet macromolecule. *Biochem. Biophys. Res. Commun.* **211**, 7–13.

Gittis, A. G., Stites, W. E. & Lattman, E. E. (1993). The phase transition between a compact denatured state and a random coil state in staphylococcal nuclease is 1st-order. *J. Mol. Biol.* **232**, 718–724.

Glaeser, R. M. & Jap, B. K. (1985). Absorption flattening in the circular dischroism spectra of small membrane fragments. *Biochemistry,* **24**, 6398–6401.

Go, K. & Parthasarathy, R. (1995). Crystal structure and a twisted β-sheet conformation of the tripeptide L-leucyl-L-leucyl-L-leucine monohydrate trimethanol solvate: conformation analysis of tripeptides. *Biopolymers,* **36**, 607–614.

Golding, C., Senior, S., Wilson, M. T. & O'Shea, P. (1996). Time resolution of binding and membrane insertion of a mitochondrial signal peptide: correlation with structural changes and evidence for cooperativity. *Biochemistry,* **35**, 10931–10937.

Gouaux, E. (1997). Channel-forming toxins: tales of transmission. *Curr. Opin. Struct. Biol.* **7**, 566–573.

Haltia, T. & Freire, E. (1995). Forces and factors that contribute to the structural stability of membrane proteins. *Biochim. Biophys. Acta,* **1241**, 295–322.

He, K., Ludtke, S. J., Huang, H. W. & Worcester, D. L. (1995). Antimicrobial peptide pores in membranes detected by neutron in-plane scattering. *Biochemistry,* **34**, 15614–15618.

Hristova, K., Selsted, M. E. & White, S. H. (1996). Interactions of monomeric rabbit neutrophil defensins with bilayers: Comparison with dimeric human defensin HNP-2. *Biochemistry,* **35**, 11888–11894.

Huschilt, J. C., Millman, B. M. & Davis, J. H. (1989). Orientation of alpha-helical peptides in a lipid bilayer. *Biochim. Biophys. Acta,* **979**, 139–141.

Jacobs, R. E. & White, S. H. (1989). The nature of the hydrophobic binding of small peptides at the bilayer interface: implications for the insertion of transbilayer helices. *Biochemistry,* **28**, 3421–3437.

Johnson, W. C. (1990). Protein secondary structure and circular dichroism: a practical guide. *Proteins: Struct. Funct. Genet.* **7**, 205–214.

Kaiser, E. T. & Kezdy, F. J. (1983). Secondary structures of proteins and peptides in amphiphilic environments (a review). *Proc. Natl Acad. Sci. USA,* **80**, 1137–1143.

Kanellis, P., Romans, A. Y., Johnson, B. J., Kercret, H., Chiovetti, R., Jr, Allen, T. M. & Segrest, J. P. (1980). Studies of synthetic peptide analogs of the amphipathic helix. *J. Biol. Chem.* **255**, 11464–11472.

Kiyota, T., Lee, S. & Sugihara, G. (1996). Design and synthesis of amphiphilic alpha-helical model peptides with systematically varied hydrophobic-hydrophilic balance and their interaction with lipid- and bio-membranes. *Biochemistry,* **35**, 13196–13204.

Kleinschmidt, J. H. & Tamm, L. K. (1996). Folding intermediates of a β-barrel membrane protein. Kinetic evidence for a multi-step membrane insertion mechanism. *Biochemistry,* **35**, 12993–13000.

Knutson, J. R., Beechem, J. M. & Brand, L. (1983). Simultaneous analysis of multiple fluorescence decay curves: A global approach. *Chem. Phys. Letters,* **102**, 501–507.

Krantz, D. D., Zidovetzki, R., Kagan, B. L. & Zipursky, S. L. (1991). Amphipathic β structure of a leucine-rich repeat peptide. *J. Biol. Chem.* **266**, 16801–16807.

Krimm, S. & Bandekar, J. (1986). Vibrational spectroscopy and conformation of peptides, polypeptides, and proteins. *Advan. Protein Chem.* **38**, 181–364.

Ladokhin, A. S., Wimley, W. C. & White, S. H. (1995). Leakage of membrane vesicle contents: Determination of mechanism using fluorescence requenching. *Biophys. J.* **69**, 1964–1971.

Ladokhin, A. S., Selsted, M. E. & White, S. H. (1997a). Bilayer interactions of indolicidin, a small antimicrobial peptide rich in tryptophan, proline, and basic amino acids. *Biophys. J.* **72**, 794–805.

Ladokhin, A. S., Wimley, W. C., Hristova, K. & White, S. H. (1997b). Mechanism of leakage of contents of membrane vesicles determined by fluorescence requenching. *Methods Enzymol.* **278**, 474–486.

Lang, E., Szendrei, G. I., Elekes, I., Lee, V. M. Y. & Otvos, L., Jr (1992). Reversible β-pleated sheet formation of a phosphorylated synthetic τ peptide. *Biochem. Biophys. Res. Commun.* **182**, 63–69.

Lee, S., Yoshitomi, H., Morikawa, M., Ando, S., Takiguchi, H., Inoue, T. & Sugihara, G. (1995). Homooligopeptides composed of hydrophobic amino acid residues interact in a specific manner by taking alpha-helix or beta- structure toward lipid bilayers. *Biopolymers,* **36**, 391–398.

Li, S.-C. & Deber, C. M. (1994). A measure of helical propensity for amino acids in membrane environments. *Nature Struct. Biol.* **1**, 368–373.

Ludtke, S. J., He, K., Wu, Y. L. & Huang, H. W. (1994). Cooperative membrane insertion of magainin correlated with its cytolytic activity. *Biochim. Biophys. Acta,* **1190**, 181–184.

MacKenzie, K. R., Prestegard, J. H. & Engelman, D. M. (1997). A transmembrane helix dimer: structure and implications. *Science,* **276**, 131–133.

Mancheño, J. M., Gasset, M., Albar, J. P., Lacadena, J., Martínez del Pozo, A., Oñaderra, M. & Gavilanes, J. G. (1995). Membrane interaction of a β-structure-forming synthetic peptide comprising the 116-139th sequence region of the cytotoxic protein α-sarcin. *Biophys. J.* **68**, 2387–2395.

Mannella, C. A. (1992). The ins and outs of mitochondrial membrane channels. *Trends Biochem. Sci.* **17**, 315–320.

Marsh, D. (1997). Dichroic ratios in polarized Fourier transform infrared for nonaxial symmetry of β-sheet structures. *Biophys. J.* **72**, 2710–2718.

Mayer, L. D., Hope, M. J. & Cullis, P. R. (1986). Vesicles of variable sizes produced by a rapid extrusion procedure. *Biochim. Biophys. Acta,* **858**, 161–168.

McIntosh, T. J. & Holloway, P. W. (1987). Determination of the depth of bromine atoms in bilayers formed from bromolipid probes. *Biochemistry,* **26**, 1783–1788.

McLaurin, J. & Chakrabartty, A. (1996). Membrane disruption by Alzheimer β-amyloid peptides mediated through specific binding to either phospholipids or gangliosides. Implications for neurotoxicity. *J. Biol. Chem.* **271**, 26482–26489.

Merutka, G. & Stellwagen, E. (1991). Effect of amino acid ion pairs on peptide helicity. *Biochemistry,* **30**, 1591–1594.

Murzin, A. G., Lesk, A. M. & Chothia, C. (1994a). Principles determining the structure of β-sheet barrels in proteins. I. A theoretical analysis. *J. Mol. Biol.* **236**, 1369–1381.

Murzin, A. G., Lesk, A. M. & Chothia, C. (1994b). Principles determining the structure of β-sheet barrels in proteins. II. The observed structures. *J. Mol. Biol.* **236**, 1382–1400.

Nitsch, R. M., Blusztajn, J. K., Pittas, A. G., Slack, B. E., Growdon, J. H. & Wurtman, R. J. (1992). Evidence for a membrane defect in Alzheimer disease brain. *Proc. Natl Acad. Sci. USA,* **89**, 1671–1675.

O'Neil, K. T. & DeGrado, W. F. (1990). A thermodynamic scale for the helix-forming tendencies of the commonly occurring amino acids. *Science,* **250**, 646–651.

Pakula, A. A. & Sauer, R. T. (1990). Reverse hydrophobic effects relieved by amino-acid substitutions at a protein surface. *Nature,* **344**, 363–364.

Parente, R. A., Nir, S. & Szoka, F. (1990). Mechanism of leakage of phospholipid vesicle contents induced by the peptide GALA. *Biochemistry,* **29**, 8720–8728.

Parker, M. W., Buckley, J. T., Postma, J. P. M., Tucker, A. D., Leonard, K., Pattus, F. & Tsernoglou, D. (1994). Structure of the *Aeromonas* toxin proaerolysin in its water-soluble and membrane-channel states. *Nature,* **367**, 292–295.

Petosa, C., Collier, R. J., Klimpel, K. R., Leppla, S. H. & Liddington, R. C. (1997). Crystal structure of the anthrax toxin protective antigen. *Nature,* **385**, 833–838.

Press, W. H., Flannery, B. P., Teukolsky, S. A. & Vetterling, W. T. (1989). *Numerical Recipes. The Art of Scientific Computing,* Cambridge University Press, Cambridge.

Rapaport, D., Peled, R., Nir, S. & Shai, Y. (1996). Reversible surface aggregation in pore formation by pardaxin. *Biophys. J.* **70**, 2502–2512.

Richardson, J. S. (1981). The anatomy and taxonomy of protein structure. *Advan. Protein Chem.* **34**, 167–339.

Roseman, M. A. (1988). Hydrophobicity of the peptide C = O···H—N hydrogen-bonded group. *J. Mol. Biol.* **201**, 621–625.

Sansom, M. S. P. & Kerr, I. D. (1995). Transbilayer pores formed by β-barrels: molecular modeling of pore structures and properties. *Biophys. J.* **69**, 1334–1343.

Sawyer, D. B., Williams, L. P., Whaley, W. L., Koeppe, R. E. & Andersen, O. S. (1990). Gramicidins A, B, and C form structurally equivalent ion channels. *Biophys. J.* **58**, 1207–1212.

Schirmer, T., Keller, T. A., Wang, Y.-F. & Rosenbusch, J. P. (1995). Structural basis for sugar translocation through maltoporin channels at 3. 1 Å resolution. *Science,* **267**, 512–514.

Scholtz, J. M., Marqusee, S., Baldwin, R. L., York, E. J., Stewart, J. M., Santoro, M. & Bolen, D. W. (1991). Calorimetric determination of the enthalpy change for the α-helix to coil transition of an alanine peptide in water. *Proc. Natl Acad. Sci. USA,* **88**, 2854–2858.

Schulz, G. E. (1996). Porins: general to specific, native to engineered passive pores. *Curr. Opin. Struct. Biol.* **6**, 485–490.

Schwarz, G. & Beschiaschvili, G. (1989). Thermodynamic and kinetic studies on the association of melittin with a phospholipid bilayer. *Biochim. Biophys. Acta,* **979**, 82–90.

Shortle, D., Meeker, A. K. & Freire, E. (1988). Stability mutants of staphylococcal nuclease: large compensating enthalpy-entropy changes for the reversible denaturation reaction. *Biochemistry,* **27**, 4761–4768.

Simon, S. M. (1995). Protein-conducting channels for the translocation of proteins into and across membranes. *Cold Spring Harbor Symp. Quant. Biol.* **60**, 57–69.

Smith, C. K. & Regan, L. (1995). Guidelines for protein design: the energetics of beta sheet side-chain interactions. *Science,* **270**, 980–982.

Smith, C. K., Withka, J. M. & Regan, L. (1994). A thermodynamic scale for the beta-sheet forming tendencies of the amino acids. *Biochemistry,* **33**, 5510–5517.

Song, L., Hobaugh, M. R., Shustak, C., Cheley, S., Bayley, H. & Gouaux, J. E. (1996). Structure of staphylococcal α-hemolysin, a heptameric transmembrane pore. *Science,* **274**, 1859–1866.

Stankowski, S. & Schwarz, G. (1990). Electrostatics of a peptide at a membrane water interface. The pH dependence of melittin association with lipid vesicles. *Biochim. Biophys. Acta,* **1025**, 164–172.

Surrey, T., Schmid, A. & Jähnig, F. (1996). Folding and membrane insertion of the trimeric β-barrel protein OmpF. *Biochemistry,* **35**, 2283–2288.

Svennerholm, L. & Gottfries, C.-G. (1994). Membrane lipids, selectively diminished in Alzheimer brains, suggest synapse loss as a primary event in early-onset form (type I) and demyelination in late-onset form (type II). *J. Neurochem.* **62**, 1039–1047.

Tamm, L. K. (1991). Membrane insertion and lateral mobility of synthetic amphiphilic signal peptides in lipid model membranes. *Biochim. Biophys. Acta,* **1071**, 123–148.

Tamm, L. K., Tomich, J. M. & Saier, M. H. (1989). Membrane incorporation and induction of secondary structure of synthetic peptides corresponding to the N-terminal signal sequences of the glucitol and mannitol permeases of *Escherichia coli*. *J. Biol. Chem.* **264**, 2587–2592.

Terzi, E., Hölzemann, G. & Seelig, A. (1994a). Reversible random coil-β-sheet transition of the Alzheimer β-amyloid fragment. *Biochemistry,* **33**, 1345–1350.

Terzi, E., Hölzemann, G. & Seelig, J. (1994b). Alzheimer β-amyloid peptide 25-35: electrosatic interactions with phospholipid membranes. *Biochemistry,* **33**, 7434–7441.

Terzi, E., Hölzemann, G. & Seelig, J. (1995). Self-association of beta-amyloid peptide (1-40) in solution and

binding to lipid membranes. *J. Mol. Biol.* **252**, 633–642.
Thorgeirsson, T. E., Yu, Y. G. & Shin, Y.-K. (1995). A limiting law for the electrostatics of the binding of polypeptides to phospholipid bilayers. *Biochemistry*, **34**, 5518–5522.
Tilstra, L. & Mattice, W. L. (1996). The β sheet ↔ coil transition of polypeptides, as determined by circular dichroism. In *Circular Dichroism and the Conformational Analysis of Biomolecules* (Fasman, G. D., ed.), pp. 261–284, Plenum Press, New York.
Tytler, E. M., Anantharamaiah, G. M., Walker, D. E., Mishra, V. K., Palgunachari, M. N. & Segrest, J. P. (1995). Molecular basis for prokaryotic specificity of magainin-induced lysis. *Biochemistry*, **34**, 4393–4401.
Venyaminov, S. Y. & Kalnin, N. N. (1990). Quantitative IR spectrophotometry of peptide compounds in water (H_2O) solutions. I. Spectral parameters of amino acid residue absorption bands. *Biopolymers*, **30**, 1243–1257.
Wang, L., O'Connell, T., Tropsha, A. & Hermans, J. (1996). Molecular simulations of β-sheet twisting. *J. Mol. Biol.* **262**, 283–293.
Wang, Z. L., Jones, J. D., Rizo, J. & Gierasch, L. M. (1993). Membrane-bound conformation of a signal peptide – a transferred nuclear overhauser effect analysis. *Biochemistry*, **32**, 13991–13999.
Weiss, M. S., Kreusch, A., Schiltz, E., Nestel, U., Welte, W., Weckesser, J. & Schulz, G. E. (1991). The structure of porin from *Rhodobacter capsulatus* at 1.8 Å resolution. *FEBS Letters*, **280**, 379–382.
White, S. H. & Wimley, W. C. (1994). Peptides in lipid bilayers: structural and thermodynamic basis for partitioning and folding. *Cur. Opin. Struct. Biol.* **4**, 79–86.
White, S. H., Wimley, W. C., Ladokhin, A. S. & Hristova, K. (1998). Protein folding in membranes: determining the energetics of peptide-bilayer interactions. *Methods Enzymol.* In the press.
Wiener, M. C. & White, S. H. (1991). Transbilayer distribution of bromine in fluid bilayers containing a specifically brominated analog of dioleoylphosphatidylcholine. *Biochemistry*, **30**, 6997–7008.
Wimley, W. C. & White, S. H. (1993a). Membrane partitioning: distinguishing bilayer effects from the hydrophobic effect. *Biochemistry*, **32**, 6307–6312.
Wimley, W. C. & White, S. H. (1993b). Quantitation of electrostatic and hydrophobic membrane interactions by equilibrium dialysis and reverse-phase HPLC. *Anal. Biochem.* **213**, 213–217.
Wimley, W. C. & White, S. H. (1996). Experimentally determined hydrophobicity scale for proteins at membrane interfaces. *Nature Struct. Biol.* **3**, 842–848.
Wimley, W. C., Selsted, M. E. & White, S. H. (1994). Interactions between human defensins and lipid bilayers: Evidence for the formation of multimeric pores. *Protein Sci.* **3**, 1362–1373.
Wimley, W. C., Creamer, T. P. & White, S. H. (1996). Solvation energies of amino acid side-chains and backbone in a family of host-guest pentapeptides. *Biochemistry*, **35**, 5109–5124.
Woody, R. W. (1994). Contributions of tryptophan side-chains to the far-ultraviolet circular dichroism of proteins. *Eur. Biophys. J.* **23**, 253–262.
Woolley, G. A. & Wallace, B. A. (1992). Model ion channels–gramicidin and alamethicin. *J. Membr. Biol.* **129**, 109–136.
Woolley, G. A., Dunn, A. & Wallace, B. A. (1992). Gramicidin-lipid interactions induce specific tryptophan side-chain conformations. *Biochem. Soc. Trans.* **20**, 864–867.
Yanagisawa, K., Odaka, A., Suzuki, N. & Ihara, Y. (1995). GM1 ganglioside-bound amyloid β-protein (Aβ): a possible form of preamyloid in Alzheimer's disease. *Nature Med.* **1**, 1062–1066.
Yang, A.-S. & Honig, B. (1995). Free energy determinants of secondary structure formation. II. Antiparallel β-sheets. *J. Mol. Biol.* **252**, 366–376.
Zhang, S. G. & Rich, A. (1997). Direct conversion of an oligopeptide from a β-sheet to an α-helix: A model for amyloid formation. *Proc. Natl Acad. Sci. USA*, **94**, 23–28.
Zimm, B. H., Doty, P. & Iso, K. (1959). Determination of the parameters for helix formation in poly-γ-benzyl-L-glutamate. *Proc. Natl Acad. Sci. USA*, **45**, 1601–1606.

Edited by D. C. Rees

(Received 2 September 1997; received in revised form 12 January 1998; accepted 13 January 1998)